

Opto 2025
Book of abstracts

Contents

1	Invited speakers	3
2	Oral presentations	8
	Session I: Sensing and imaging	8
	Session II: Pulsed lasers	12
	Session III: Optical fibers	17
	Session IV: Astronomical Instruments	22
	Session V: Machine learning adaptive	24
	Session VI: Materials	27
3	Poster session	33

Invited speakers

Šárka Němcová

Title: Designing a custom ophthalmoscope: from optical simulation to functional prototype

Abstract: This talk presents the development of a fully custom ophthalmoscope — designed, prototyped, and assembled from scratch at the Czech Technical University in Prague (CTU). Starting from core optical requirements for retinal imaging, the design process combined Zemax simulations, GRIN lens integration, and precision 3D printing to produce a compact and functional device. Key challenges such as illumination geometry, optical alignment, and image quality optimization were addressed through iterative prototyping and testing. The project showcases how accessible technologies can be harnessed to create sophisticated medical instruments in a university research environment. Practical insights, lessons learned, and potential clinical applications will be shared.

Karen Volke-Sepulveda

Title: Structured waves and their interaction with matter

Abstract: Wave fields may exhibit a complex structure in intensity, phase and polarization, and this structure becomes very relevant in their interaction with matter, due to the associated dynamical properties. For example, in radiation traps, when considering small particles with respect to the wavelength, the equilibrium positions depend on the properties of the particle and the medium, while the potential energy landscape is entirely determined by the incident wave field. In contrast, large particles add a significant scattered field, causing the effective structure of the energy potential to become particle-dependent, which implies that two particles of identical properties find different equilibrium positions depending on their size. This is a general feature of radiation traps generated with structured wave fields, known at present as the particle size effect, which will be discussed using examples in optics and acoustics.

Grzegorz Soboń

Title: Ultrashort laser pulses from a lunchbox - how to make femtosecond laser simple, robust and affordable

Abstract: This talk will explore ultrashort laser pulse generation using optical fiber technology. We will discuss recent advances enabling few-cycle pulses and their applications highlighting, fiber lasers' accessibility for non-experts in fields like medicine and industrial applications. Additionally, we will explore the emerging role of AI-driven optimization algorithms in shaping and controlling ultrashort laser pulses for enhanced performance and tailored applications.

Clara Saraceno

Title: High average power Terahertz sources for time domain spectroscopy

Abstract: Ultrafast laser-driven terahertz sources are gaining in popularity in an increasingly wide range of scientific and technological applications. However, many fields continue to be severely limited by the typically low average power of these sources, which restricts speed, signal-to-noise ratio, and dynamic range in numerous measurements. Conversely, the past two decades have seen spectacular progress in high average power ultrafast laser technology based on Ytterbium lasers, rendering hundreds of watts to kilowatts of average power available to this community to drive THz sources. This has opened up the young field of high-average-power laser-driven THz time-domain spectroscopy, which promises to revolutionize many of the application fields of THz-TDS. We discuss this young field and emphasize recent advancements in broadband terahertz sources utilizing high-power ultrafast lasers as drivers, which are nearing watt-level average power. We discuss various approaches explored thus far, current challenges, future prospects for scaling, and the new opportunities these sources may open up in the future.

Daniel Urrego

Title: Demonstration of experimental schemes for imaging and sensing: from quantum to classical and back

Abstract: The experimental schemes put forward in this talk are based on simulating specific aspects of quantum concepts using classical Optics. The last scheme takes the opposite direction. In the first part, the first scheme introduces a proof-of-concept demonstration of an optical gate that uses light beam with orbital angular momentum. Inspired by the quantum fingerprinting protocol. In the second scheme employing quantum techniques, it develops the quantum version of a Differential Interference Contrast (DIC) microscope. The last scheme is a version using SU(11) that can enhance the sensitivity of the Optical Coherence tomography.

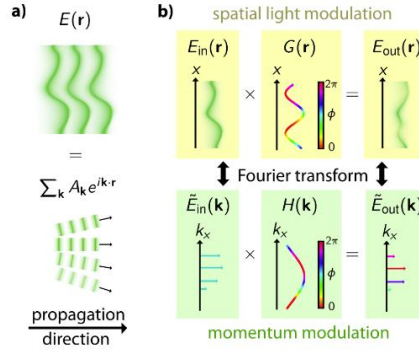
Bragging... a story of diffraction and unitary operations

Nicholas J. Sorensen¹, Michael. T. Weil¹, Arman Mansouri¹ Manuel F. Ferrer Garcia¹, and J. S. Lundeen¹

¹Department of Physics, University of Ottawa, 25 Templeton, Ottawa, K1N 6N5, ON, Canada

The ability to transform an optical field is fundamental to sensing, microscopy, telecommunication, and a myriad of other applications in optics. Typically, these transformations are performed by local optics elements, i.e. the output field at any position solely depends on the input field at the same position. Nevertheless, optical transformations using local optics are constrained to a subset of the generalized transformation. Here, we present the concept of momentum-space modulation as a platform to design and construct optical elements with nonlocal responses. In addition, we propose their implementation

using superpositions of volume holographic gratings to realize arbitrary momentum-dependent transformations of light. We introduce an analytical framework for computing the spatially varying refractive index profile of a volume hologram from a target phase transformation. In addition, we introduce an experimental implementation for writing multiplexed volume holograms allowing us to generate non-local unitary operations.



References

- [1] O. Reshef, M. P. DelMastro, K. K. Bearne, et al., “An optic to replace space and its application towards ultra-thin imaging systems,” 227 Nat. Commun. 12, 8–15 (2021).
- [2] J. T. R. Page, O. Reshef, R. W. Boyd, and J. S. Lundeen, “Designing high-performance propagation-compressing spaceplates using thin-film multilayer stacks,” Opt. Express 30, 2197 (2022)
- [3] H. Kogelnik, “Coupled wave theory for thick hologram gratings,” Bell Syst. Tech. J. 48, 2909–2947 (1969).255

Synthesis of mid-infrared fiber laser spectral lines for multi-gas detection

Yazhou Wang^{1*}, J. Enrique Antonio-Lopez², Rodrigo Amezcua-Correa², and Christos Markos¹

¹. DTU Electro, Technical University of Denmark, 2800 Kgs. Lyngby, Denmark

². CREOL, The College of Optics and Photonics, University of Central Florida, Orlando, Florida 32816, USA

Corresponding author: yazwang@dtu.dk

The synthesis of multiple narrow optical spectral lines, precisely and independently tuned across the near- to mid-infrared region, is a pivotal research area that enables selective and real-time detection of trace gas species within complex gas mixtures. However, existing methods for developing such light sources suffer from limited flexibility and low pulse energy, particularly in the mid-infrared domain. Here, we introduce a concept that is based on the combination of an appropriate design of near-infrared fiber laser pump and cascaded configuration of gas-filled anti-resonant hollow-core fiber (ARHCF) technology. This concept enables the synthesis of multiple independently tunable spectral lines, with $>1 \mu\text{J}$ high pulse energies and a few nanoseconds pulse width in the near- and mid-infrared regions. The number and wavelengths of the generated spectral lines can be dynamically reconfigured. A proof-of-concept laser beam synthesized of two narrow spectral lines at $3.99 \mu\text{m}$ and $4.25 \mu\text{m}$ wavelengths is demonstrated and combined with photoacoustic modality for real-time SO_2 and CO_2 detection.

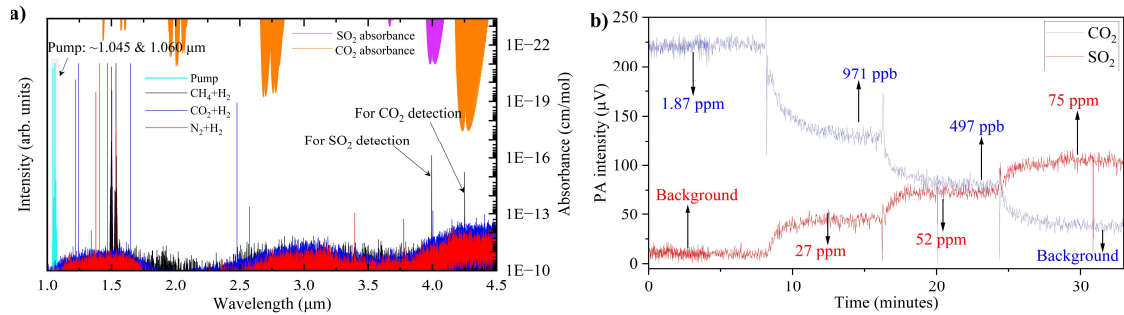


Fig. 1 (a) Wavelength conversion examples through filling different gas (CH_4 , CO_2 and N_2) into the 1st stage ARHCF. The 2nd stage ARHCF is constantly filled with H_2 at 30 bar. Left axis shows measured optical spectra including pump lines, and Raman lines output from the H_2 -filled 2nd stage ARHCF. Right axis shows the absorbance spectra of CO_2 and SO_2 obtained from the high-resolution transmission molecular absorption database (HITRAN). (b) Real-time photoacoustic detection of CO_2 and SO_2 using the synthesized spectral lines at 3.99 and $4.25 \mu\text{m}$ in (a).

The center part of the proposed method is a cascaded silica ARHCF configuration pumped by a near-IR laser with multiple synthesized reconfigurable spectral lines lying within the gain range of Yb-doped fiber amplifier [1]. The wavelengths of these synthesized pump lines are nonlinearly converted based on the rotational/vibrational stimulated Raman scattering (SRS) effect of gases filled in the 1st and 2nd stage ARHCFs. As a result, the synthesized Raman Stokes lines have diverse wavelengths from the near- to mid-IR region. While any pump wavelength can be selected, we specifically select two pump lines at ~ 1044 and $\sim 1060 \text{ nm}$. Figure 1a shows the diversity of the generated and synthesized Raman lines over a broad IR range from 1.2 to $4.3 \mu\text{m}$, achieved by filling 30 bar H_2 into the 2nd stage ARHCF while the 1st stage ARHCF is filled with different gases such as CH_4 , CO_2 , and N_2 . For example, synthesized nanosecond Raman laser lines at 3.99 and $4.25 \mu\text{m}$ are generated in the case of filling CH_4 into the 1st stage ARHCF. The maximum pulse energies are measured to be $1.7 \mu\text{J}$ at $3.99 \mu\text{m}$ and $2.7 \mu\text{J}$ at $4.25 \mu\text{m}$, respectively, at 30 bar H_2 pressure. Their linewidths are measured to be $\sim 1.3 \text{ nm}$, and their wavelength and independently and precisely tunable through tuning the pump laser. Another example is to filling CO_2 into the 1st stage ARHCF, which, due to the cascaded vibrational SRS effect of CO_2 , leads to the generation of four mid-IR Raman lines within a broad spectral range at 2478 , 2574 , 3778 , and 4004 nm , respectively.

The Raman laser beam consisting of synthesized 3.99 and $4.25 \mu\text{m}$ Raman spectral lines is collimated by a CaF_2 lens with a 3 cm focal length and then coupled into a resonant acoustic chamber for SO_2 and CO_2 detection. SO_2 and CO_2 mixture diluted by pure Ar flows through the acoustic chamber for validating the proposed detection approach. Their concentrations are independently varied adjusted by with mass flow controllers (MFCs). Figure 3d shows the measured PA intensity at different CO_2 and SO_2 concentrations in ppm and ppb level. The detection limit is estimated to be 329 ppb for CO_2 and 19 ppm for SO_2 at 1 kHz laser repetition rate [1].

Funding and acknowledgements. This work is supported by the Danmarks Frie Forskningsfond Hi-SPEC project (Grant No. 8022-00091B), VILLUM Fonden (Grant No. 36063, Grant No. 40964), LUNDBECK Fonden (Grant No. R346-2020-1924, R276-2018-869), and US ARO (Grant No. W911NF-19-1-0426).

References

[1] Y. Wang, *et al.* "Synthesizing gas-filled anti-resonant hollow-core fiber Raman lines enables access to the molecular fingerprint region". Nat. Commun. 15, 9427(2024).

Oral presentations

Real-time clustering of hyperspectral data in multiphoton microscopy

Maciej Barna^a, Katarzyna Kunio^a, Grzegorz Soboń^a, Jakub Boguslawski^a

^aLaser & Fiber Electronics Group, Faculty of Electronics, Photonics and Microsystems,
Wrocław University of Science and Technology, Wybrzeże Wyspiańskiego 27, 50-370 Wrocław, Poland
Corresponding author: maciej.barna@pwr.edu.pl

Hyperspectral two-photon microscopy is a powerful fluorescence imaging technique, however its applicability outside laboratory conditions is limited due to the high cost of spectral detectors. To address this, a simplified version of the microscope was developed, which records data directly in the phasor domain, replacing the spectrometer with two optical filters [1]. Spectral phasor represents complex hyperspectral signals as a set of points inside a unit circle, where peak wavelength is encoded with angle and full width at half maximum (FWHM) with magnitude [2]. Example phasor data are presented in Fig. 1a. However, existing methods for analyzing phasor data do not allow for real-time processing. In this work, we present a method that significantly accelerates the analysis of fluorescence data while maintaining accuracy.

Clustering is a major goal in fluorescence data analysis. It involves segmenting the image based on the optical spectra recorded at individual pixels. In the case of phasor data, clustering is performed based on the spectral phasor coordinates. One of the more popular clustering methods is the k-means algorithm [3], which iteratively groups the data by minimizing the sum of squared distances between points and cluster centers. The method we propose accelerates the identification of cluster centers by searching for density peaks on its histogram (discretized phasor plot with values assigned to bins that represent number of data points inside, example presented in Fig 1b) and then grouping phasor points using the inverse distance weighting (IDW) algorithm [4]. Figure 1c shows simplified flowchart of the proposed method.

To compare both methods, synthetic data simulating the presence of two fluorophores in an image were used. Most pixels contained only one fluorophore, but some of them had mixture of both in variable proportions. Fluorophore which contributes in 50% or more is regarded to as a dominant fluorophore. Example spectra of the generated fluorophores are shown in Fig. 1d. The methods were tested for different spectral separations ($\Delta\lambda$) ranging from 20 to 80 nm; an example for $\Delta\lambda = 20$ nm is shown below. Fig. 1e presents a reference image, where the pixel color indicates the dominant fluorophore (orange - fluorophore a, red - fluorophore b). The clustering results obtained using the k-means and IDW methods are shown in Figs. 1f and 1g, respectively.

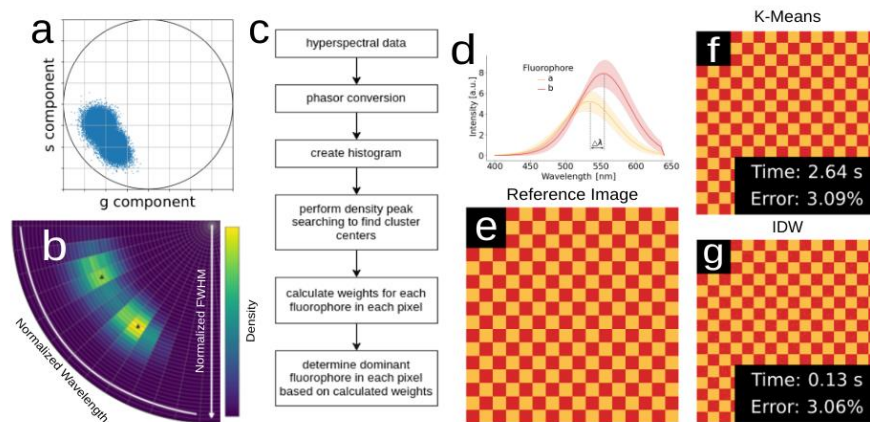


Fig. 1: (a) example phasor data, (b) histogram created from example phasor data with marked centers, (c) flowchart of the proposed method, (d) example optical spectra of the generated fluorophores ($\Delta\lambda = 20$ nm), (e) ground truth pattern for comparing clustering results, (f) clustering results obtained using the k-means method, (g) and using the IDW method.

Obtained results show that the proposed method accelerated the clustering of hyperspectral data while maintaining comparable accuracy. Both methods achieved an accuracy level above 96%, however the k-means method required 2.64 s to produce results, whereas the IDW method took only 0.13 s, representing over a 20-fold reduction in computation time. This time reduction was made possible by replacing iterative searching for cluster centers with histogram analysis. The application of this method enables real-time visualization of clustering results.

Funding and acknowledgements. National Science Centre, Poland (2021/43/D/ST7/01126).

References

- [1] N. Hedde, R. Cinco, L. Malacrida, A. Kamaid, E. Gratton, "Phasor-based hyperspectral snapshot microscopy allows fast imaging of live, three-dimensional tissues for biomedical applications", *Commun. Biol.* 4(1), 501 (2021).
- [2] L. Malacrida, E. Gratton, D. M. Jameson, "Model-free methods to study membrane environmental probes: a comparison of the spectral phasor and generalized polarization approaches", *Methods Appl. Fluoresc.* 3, 047001 (2015).
- [3] J. Macqueen, "Some methods for classification and analysis of multivariate observations", *Berkeley Symp. Math. Statist. Prob.* 1, 281-297 (1967).
- [4] D. W. S. Wong, "Inverse distance weighting", *Int. Encycl. Geogr.: People, Earth, Environ. Technol.*, 1-7 (2017).

Spectral Tomography Analysis of Transverse Modes in VCSELs with Broken Symmetry Apertures

M. Betke¹, A. N. Piasecka¹, M. GebSKI², J. A. Lott³, T. Czyszanowski² and M. Pieczarka¹

¹Department of Experimental Physics, Faculty of Fundamental Problems of Technology, Wrocław University of Science and Technology, Wyb. Wyspiańskiego 27, 50-370 Wrocław, Poland

²Institute of Physics, Lodz University of Technology, ul. Wólczajska 217/221, 93-005 Łódź, Poland

³Institute of Solid State Physics and Center of Nanophotonics, Technical University Berlin, Hardenbergstraße 36, 10623 Berlin, Germany

Corresponding author: *mateuszbetke2275@gmail.com

Vertical-cavity surface-emitting lasers (VCSELs) with chaotic cavities have attracted attention because of their enhanced quantum efficiency, coherence, and stability [1-3]. This study focuses on the spectral tomography of transverse modes in VCSELs with broken symmetry apertures, with the aim of investigating spatial lasing characteristics and output efficiencies.

We conducted a analysis of individual modes in VCSELs with circular and crescent-shaped apertures, utilizing both near-field and far-field measurements. Using spectral tomography, we reconstructed the intensity distribution of the modes, revealing the non-trivial nature of the broken symmetry aperture. Our findings indicate that breaking the symmetry can lead to a more uniform spatial lasing distribution, which is crucial for applications requiring stable and homogeneous emission.

Furthermore, we compared the current characteristics and output efficiencies (Fig. 1) of the devices, highlighting the advantages of the chaotic aperture. Spectral tomography provides valuable insight for the design and optimization of chaotic laser systems. The study underscores the potential of non-symmetric VCSELs for practical applications, owing to their superior stability and homogeneity. However, further research is necessary to validate the multimodal emission stability of chaotic cavities and to explore the dynamics of lasers with broken-symmetry apertures in comparison to circular aperture characteristics.

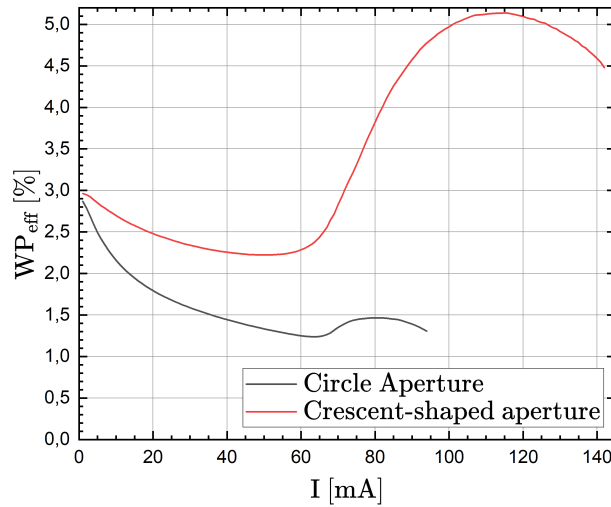


Fig. 1: Wall-Plug Efficiency $WP_{eff} = \frac{P_{opt}}{P_{el}} = \frac{P_{opt}}{U \cdot I}$ as a function of supply current, for a pair of lasers with apertures of similar area.

Funding and acknowledgments. The research was carried out under the SONATA 16 grant of the National Science Centre (No. 2020/39/D/ST3/03546) entitled "Thermalization, interactions and Bose-Einstein condensation of photons in semiconductor microcavity lasers", headed by Maciej Pieczarka.

References

- [1] S. Bittner, S. Guazzotti, Y. Zeng, X. Hu, H. Yilmaz, K. Kim, S. S. Oh, Q. J. Wang, O. Hess, and H. Cao, "Suppressing spatio-temporal lasing instabilities with wave-chaotic microcavity lasers", *Science* **361**, 1225 (2018).
- [2] A. Brejnak, M. GebSKI, A. K. Sokół, M. Marciniak, M. Wasiak, J. Muszalski, J. A. Lott, I. Fischer, and T. Czyszanowski, "Boosting the output power of large-aperture lasers by breaking their circular symmetry", *Optica* **8**, 1167 (2021).
- [3] Omar Alkhazragi, Ming Dong, Liang Chen, Dong Liang, Tien Khee Ng, Junping Zhang, Hakan Bagci, and Boon S. Ooi, "Modifying the coherence of vertical-cavity surface-emitting lasers using chaotic cavities", *Optica* **10**, 191-199 (2023)

Refractive index sensor utilizing long tapered side-hole optical fiber

Rafal Kosturek*, Michał Dudek, Leszek R. Jaroszewicz

Institute of Applied Physics, Military University of Technology, ul. gen. Sylwestra Kaliskiego 2, 00-908 Warsaw, Poland

The field of fiber optic technology has rapidly evolved, giving rise to a broad spectrum of sensors applicable in both chemical and biochemical environments. One significant advancement is the development of tapered optical fibers, which exhibit enhanced sensitivity and versatility [1]. These optical elements enables the detection of various external factors, including the refractive index (RI) [2]. By selecting appropriate process parameters, it is possible to fabricate tapers with different tapered region lengths, which determines their sensing properties. The tapering process can be applied to standard single-mode fibers (SMFs) and specialty fibers with significantly more complex internal structures [3] [4]. The presented technological work was carried out on side-hole optical fiber (S-H OF), characterized by an elliptical core and two air tunnels running in close proximity to the core (Fig. 1 (b)). The low-pressure flame technique was used to fabricate the tapers, which enabled the production of 20 mm long tapers while preserving the internal structure of the fiber. The obtained taper was investigated for external RI detection using immersion liquids in the range of 1.32–1.42 RIU. The measurements were conducted in two spectral ranges: 600–1200 nm and 1200–1800 nm, using a supercontinuum light source and an optical spectrum analyzer. Figure 1(a) presents the spectral analysis for five selected RI values within the narrowed range of 1270–1350 nm.

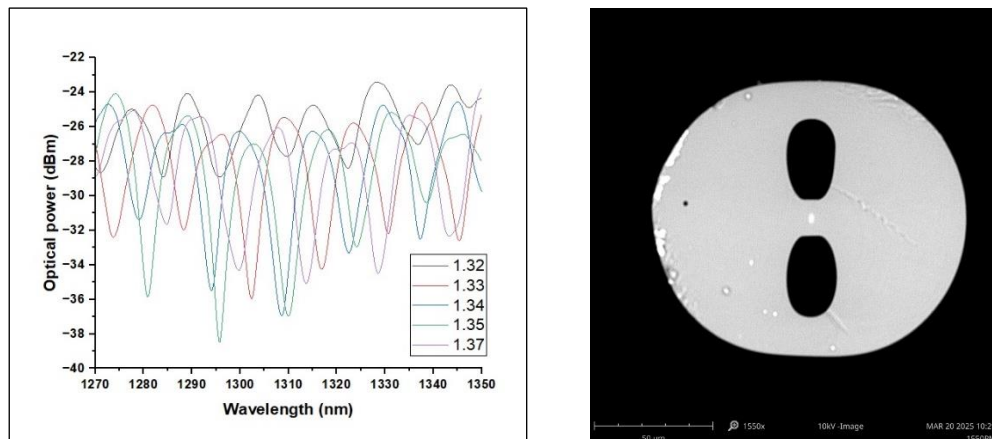


Fig. 1 (a) The obtained spectral response for immersion liquids with five representative RI values in the wavelength range of 1270-1350 (b) Internal structure of utilized S-H OF.

Spectral analysis revealed characteristic interference dips whose positions shifted linearly toward longer wavelengths with increasing external RI. The highest sensitivity was recorded in the near-infrared region (1270–1380 nm), with values reaching up to 591.8 nm/RIU. In the visible range (600–690 nm), the maximum sensitivity observed was 155.9 nm/RIU. These results highlight that the sensitivity of the sensor increases with wavelength, attributed to stronger evanescent field interaction at longer wavelengths, especially in the tapered fiber region where mode field extension is enhanced. The study confirms that long tapered S-H OFs can serve as effective platforms for RI sensing via spectral interrogation, showing competitive sensitivity compared to other fiber-optic sensor designs. While not as sensitive as interferometric or plasmonic structures, the approach benefits from structural simplicity and potential for miniaturization. Future improvements could include temperature compensation, mechanical stabilization, and integration with selective coatings or functionalized materials applied onto tapered S-H OF structures to expand the range of chemical or biosensing applications.

Funding and acknowledgements. This research was financially supported by the Military University of Technology under research project UGB - 531-000031-W900-22. The S-H OF used in the research was kindly provided by the Laboratory of Optical Fibers Technology at Maria Curie-Skłodowska University in Lublin, Poland.

References

- [1] S. Korposh, S.W. James, S.-W. Lee, R.P. Tatam. “Tapered Optical Fibre Sensors: Current Trends and Future Perspectives”. *Sensors* 19(10), 2294 (2019).
- [2] E. Ujah, M. Lai, G. Slaughter. “Ultrasensitive tapered optical fiber refractive index glucose sensor”. *Sci Rep.* 13, 4495 (2023).
- [3] N.A Salman “Preparation of tapered photonic crystal fiber material to employ the evanescent wave for sensing applications”. *Materials Today: Proceedings*, 61(3), 681-685 (2022).
- [4] A. Li, Y. Zhao. “A Mach-Zehnder interferometer based on tapered dual side hole fiber for refractive index sensing” *Opt. Fiber Tech.*, 45, 267-270 (2018)

Terahertz Frequency Comb mapping with Rydberg Atom Sensors

Wiktor Krokosz,^{1,2,*} Jan Nowosielski,^{1,2} Bartosz Kasza,^{1,2} Sebastian Borówka,^{1,2} Mateusz Mazelanik,^{1,2} Wojciech Wasilewski,^{1,2} and Michał Parniak^{1,2}

1. Centre for Quantum Optical Technologies, Centre of New Technologies, University of Warsaw, Banacha 2c, 02-097 Warsaw, Poland
2. Faculty of Physics, University of Warsaw, Pasteura 5, 02-093 Warsaw, Poland

Corresponding author: *w.krokosz@cent.uw.edu.pl

Rydberg atoms, known for their extreme atomic properties and high sensitivity to external electric fields, offer a revolutionary approach to RF field measurement. Their quantum nature enables direct electric field sensing, self-calibration, broad frequency tunability, and other advantages over conventional methods [1]. Advances in hot Rydberg atomic vapor systems have demonstrated remarkable sensitivity, paving the way for applications in imaging and single-photon detection [2].

Quantum measurements in the RF domain have traditionally been hindered by significant attenuation and diffraction effects due to long wavelengths. By utilizing six-wave mixing in a Rubidium vapor cell, we achieved efficient upconversion to the optical domain, thus extending RF quantum sensing capabilities into the optical spectrum. Implementing a single-photon counter in our setup allowed us to measure field amplitudes at the thermal limit, overcoming the limitations of standard two-photon Rydberg electrometry.

Building on this success, we explored higher frequencies, particularly the challenging terahertz (THz) range, which is undergoing rapid development due to its potential applications in imaging and molecular spectroscopy. Effective detection techniques are as crucial as THz generation, and Rydberg atoms provide a promising solution for sensing frequencies beyond 1 THz by simply tuning the optical excitation wavelengths.

To further enhance detection, we leveraged commercially available mmWave radar chips and photoconductive antennas (PCAs) for upconversion, addressing polarization and phase-matching challenges through custom 3D-printed metamaterials. Our setup, incorporating beam manipulation, absolute calibration, and polarization control [3], successfully resolved individual comb teeth in the THz spectrum and demonstrated a bandwidth exceeding 1.2 GHz. This room-temperature Rydberg sensor represents a major advancement over conventional cryogenic or bulky THz detectors.

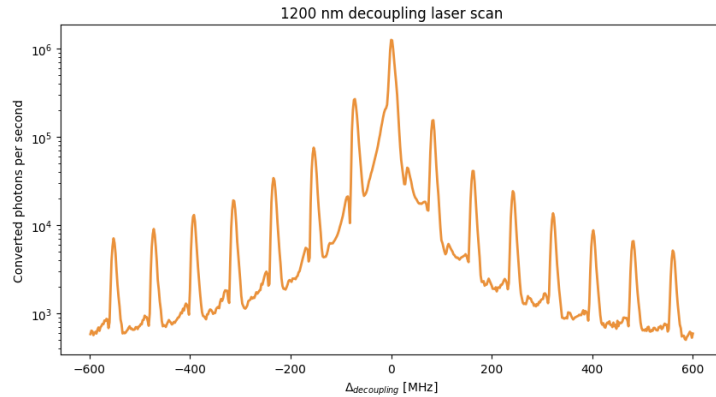


Fig. 1: Measured photon counts with respect to the detuning of the decoupling laser. Changing the detuning allows for addressing specific teeth of the THz frequency comb, which are spaced by approximately 80 MHz, corresponding to the femtosecond laser repetition rate. The counts decrease the more off resonant a tooth is, however, the measured bandwidth is large and requires further exploration.

Funding and acknowledgements. We thank M. Lipka for his initial contribution to the construction of the pulsed THz source. This research was funded in whole or in part by National Science Centre, Poland grants No. 2021/41/N/ST2/03114 and No. 2024/53/N/ST7/02730. The "Quantum Optical Technologies" (FENG.02.01-IP.05-0017/23) project is carried out within the Measure 2.1 International Research Agendas programme of the Foundation for Polish Science co-financed by the European Union under the European Funds for Smart Economy 2021-2027 (FENG).

References

- [1] H. Zhang et al. "Rydberg atom electric field sensing for metrology, communication and hybrid quantum systems". *Science Bulletin* **10**, 1515-1535 (2024).
- [2] S. Borówka et al. "Continuous wideband microwave-to-optical converter based on room-temperature Rydberg atoms". *Nature Photonics* **18**, 32-38 (2024).
- [3] S. Borówka et al. "Rydberg-atom-based system for benchmarking millimeter-wave automotive radar chips". *Phys. Rev. Appl.* **22**, 34-67 (2024).

Interferometric characterization of optical pulses in Fabry-Pérot laser diodes

Adrian F. Chlebowski^{1,*}, Jakub Mnich¹, Lukasz A. Sterczewski¹, Jaroslaw Sotor¹

*1. Group of Laser and Fiber Electronics, Faculty of Electronics, Photonics and Microsystems
Wrocław University of Science and Technology, Wybrzeże Wyspińskiego 27, 50-370 Wrocław, Poland*

Corresponding author: *adrian.chlebowski@pwr.edu.pl

Characterization of the duration and shape of optical pulses is indispensable in many practical applications such as time-resolved spectroscopy and material processing. Conventional measurement techniques utilize second-order nonlinearity in bulk crystals to produce a signal proportional to the square of the intensity. The prime example is the phenomenon of second harmonic generation (SHG), but it is limited by the requirements for phase matching and polarization compatibility in the crystal. Similar functionality can be achieved without these limitations by relying on third-order nonlinearities in two-photon absorption (TPA) [1]. A particularly strong TPA effect is observed in Fabry-Pérot (FP) laser diodes, but there is a lack of systematic studies as to their dispersive properties, residual linear absorption and detectability in nonlinear interferometry systems for pulse characterization. This niche motivates our research into the application of TPA-effect FP diodes for reliable distortion-free characterization of femtosecond pulses, which we compare with autocorrelations performed with a conventional autocorrelator with second harmonic generation in crystals (Fig. 1).

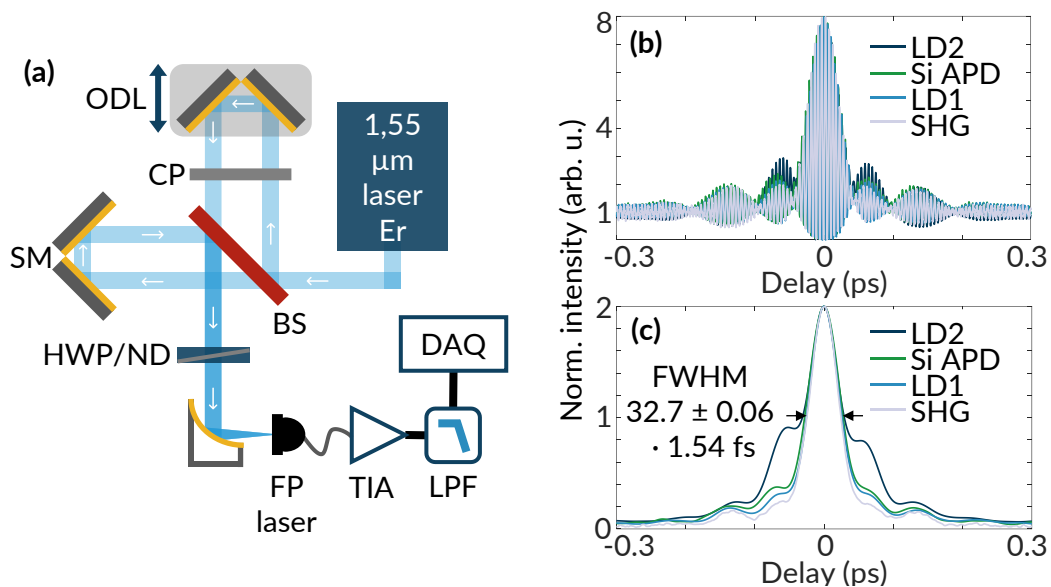


Fig. 1: (a) Michelson interferometer. ODL - optical delay line, CP - compensating plate, SM - stationary mirror, BS - beamsplitter, HWP - half-wave plate, ND - neutral density filter, TIA - transimpedance amplifier, DAQ - data acquisition (b, c) Interferometric autocorrelation and intensities for different TPA detectors and a commercial autocorrelator.

Autocorrelations obtained with an InGaAsP-based laser diode (LD1, 1.3 μm emission wavelength) in a Michelson interferometer system (Fig. 1a) overlap with SHG-based autocorrelations (Fig. 1b), demonstrating the suitability of such devices for characterizing fs pulses at telecom wavelengths. The deviation occurs in the case of short-wavelength (~ 950 nm) LD2, based on AlGaAs, whose waveguide dispersion introduces pulse distortion. Selection of an appropriate TPA detector is fundamental to achieving reliable pulse characterization. In addition, we discovered a new, previously unexplored feature of these semiconductor devices that allows simultaneous measurement of linear and nonlinear interferometric autocorrelation. The built-in InGaAs photodiode, which nominally functions as a monitor for the LD, can be used to study first-order (linear) interference along with quadratic interference measured by the LD. This feature is of practical significance in techniques to reconstruct the pulse time profile.

Funding and acknowledgements. The research was funded by the National Science Center (NCN, Poland) under Grant No. 2022/45/B/ST7/03316. The work is supported by the use of the infrastructure of the National Laboratory of Photonics and Quantum Technologies (NPLQT), funded by European Funds under the Intelligent Development Operational Program.

References

[1] J.M. Dudley, et al., Commercial Semiconductor Devices for Two Photon Absorption Autocorrelation of Ultrashort Light Pulses, Appl. Opt. 37 (1998) 8142. <https://doi.org/10.1364/AO.37.008142>.

Carrier-envelope Offset Frequency Stabilization in a Cr:ZnS Mode-locked Laser

Jakub Jaworski*, Maciej Kowalczyk

Faculty of Electronics, Photonics and Microsystems, Wrocław University of Science and Technology, Wybrzeże Wyspiańskiego 27, 50-370 Wrocław, Poland

Corresponding author: *252929@student.pwr.edu.pl

Solid-state lasers based on chromium (Cr)-doped zinc sulfide (ZnS) or zinc selenide (ZnSe) crystals can be used to generate ultrashort ~ 30 fs pulses in a short-wavelength mid-infrared spectral region ($\sim 2.3\mu\text{m}$) [1]. Such pulsed lasers are desirable in many applications, e.g. in spectroscopy, where light source stability is a key parameter and stabilization to an optical frequency comb is often required. For the latter, stabilization of carrier-envelope offset frequency (f_{ceo}) is a crucial step. It has been shown that Cr:ZnS/Se oscillators can be exceptionally stable with the f_{ceo} phase noise of the order of 5.9 mrad [2], which mainly depends on the noise of the employed pumping source [2-4].

In this paper, we present a Cr:ZnS laser oscillator with additional setups for f_{ceo} detection and stabilization. The scheme of the experimental setup is shown in Fig. 1a. The laser output undergoes spectral broadening via self-phase modulation (SPM) in a single TiO₂ bulk plate. Detection of the f_{ceo} detection signal is performed in a f - $2f$ interferometer, which uses generation of second harmonic (SHG) in a periodically-poled lithium niobate (PPLN) crystal. Subsequently, f_{ceo} stabilization is performed in a phase-locked loop including a PID regulator, which controls the power of the pump laser.

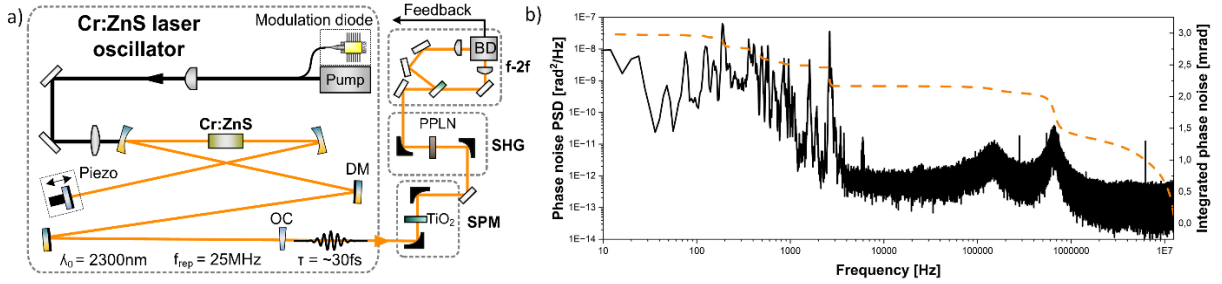


Fig. 1 (a) Experimental setup for detection and stabilization of carrier-envelope offset frequency (DM – dispersive mirror, OC – output coupler, SPM – spectral broadening, SHG – second harmonic generation, BD – balanced detector). (b) Phase noise (solid line) and integrated phase noise (dashed line) measured for a stabilized Cr:ZnS laser.

Fluctuations of f_{ceo} were measured with an additional out-of-loop f - $2f$ interferometer using laser beam after spectral broadening. The results are shown in Fig. 1b. The phase noise was measured to be 3 mrad when integrating from 10 Hz up to the Nyquist limit of 12.5 MHz, representing a two times improvement when compared to previously presented best result for Cr:ZnS/Se lasers [2]. This unprecedented stability was achieved thanks to an ultra-low-noise erbium-doped fiber amplifier employed for pumping, which allowed for minimization of amplitude fluctuations of the mode-locked Cr:ZnS laser.

Funding and acknowledgements

Narodowa Agencja Wymiany Akademickiej (BPN/PPO/2022/1/00028); Max-Planck-Gesellschaft (Max Planck Partner Group Programme); The project “Ultrastable pulsed lasers covering the spectral range from near to far infrared” (FENG.02.02-IP.05-0069/23) is carried out within the First Team programme of the Foundation for Polish Science co-financed by the European Union under the European Funds for Smart Economy 2021-2027 (FENG).

References

- [1] S. B. Mirov et al., “Frontiers of mid-IR lasers based on transition metal doped chalcogenides,” IEEE J. Sel. Top. Quantum Electron. 24, 1601829 (2018).
- [2] M. Kowalczyk et al., “Ultra-CEP-stable single-cycle pulses at 2.2 μm ,” Optica 10, 801-811 (2023).
- [3] A. Barh et al., “High-power low-noise 2-GHz femtosecond laser oscillator at 2.4 μm ,” Opt. Express 30, 5019–5025 (2022).
- [4] S. Vasilyev et al., “Ultra-Low Noise Cr:ZnS Laser Source for High Performance Dual Comb Spectroscopy,” in CLEO 2024 (Optica Publishing Group, 2024), paper SM1H.4.
- [5] M. Kowalczyk et al., “SESAM-assisted Kerr-lens mode-locked Cr:ZnS laser,” Opt. Lett. 49, 5184-5187 (2024)

Analysis of input pulse parameters on gain managed nonlinear amplification regime

Mikołaj Krakowski*, Grzegorz Sobon

aser & Fiber Electronics Group, Faculty of Electronics, Photonics and Microsystems, Wrocław University of Science and Technology,
Wybrzeże Wyspińskiego 27, 50-370 Wrocław, Poland

Corresponding author: *mikolaj.krakowski@pwr.edu.pl

Fiber lasers offer several benefits compared to traditional free-space lasers, such as small size, improved thermal management, superior beam quality, and obviating the need for alignment [1-2]. However, fiber laser systems exhibit a significant level of nonlinearity, leading to nonlinear effects that restrict their utility in high-power scenarios. While the Chirped Pulse Amplification (CPA) technique has shown promising outcomes, it suffers from gain-narrowing phenomena; the currently promising approach is the Gain Managed Nonlinear Amplification (GMN) regime [3]. In this configuration, the active fiber is considerably longer than in standard fiber amplifiers, which allows the pulses to transition through amplification regimes: at the beginning nonlinearly with significant and complex spectral broadening, progressing to a self-similar state, and reaching the GMN regime at greater length. The generation of the GMN regime relies on the spectral broadening of the pulse within the normal dispersion regime, thus specific fibers and fiber lengths are required.

The literature highlights several benefits of the GMN amplification regime - high output power, a broad optical spectrum of the emitted pulse, and the compressibility with diffraction gratings to less than 30 fs. However, it is also noted that the amplifier's performance is significantly influenced by the chirp of the input pulse [3], even though this regime is believed to be a nonlinear attractor. This research offers a comprehensive analysis of how the GMN amplifier responds to various parameters of the seeding pulse. Figure 1. a) depicts a simplified schematic of the experimental setup. This setup features a femtosecond oscillator that emits at a wavelength of 1560 nm; post-amplification, the pulse experiences a spectral blue-shift in a highly nonlinear HNLF fiber due to the production of a dispersion wave, ultimately resulting in an 80-nm-wide spectrum spanning from 1010 to 1090 nm. From this range, three specific wavelengths (1020, 1030, 1040 nm) and three spectral widths (8, 6, and 4 nm) were selected for analysis. These filtered pulses were introduced into a 3.4-meter-long ytterbium-doped double-clad fiber (Coherent PLMA-YDF-10/125-VIII), which was pumped by a 976-nm laser at 10W. The study focused on assessing the amplifier's response (output pulse spectrum) for compressed as well as two stretched input pulses (both negative and positive chirp). Figure 1. b) presents selected optical spectra for input pulses with a width of 4 nm, detailing the spectra for both the compressed pulse and the stretched pulse within the compressor, with an average pulse power of 2 mW.

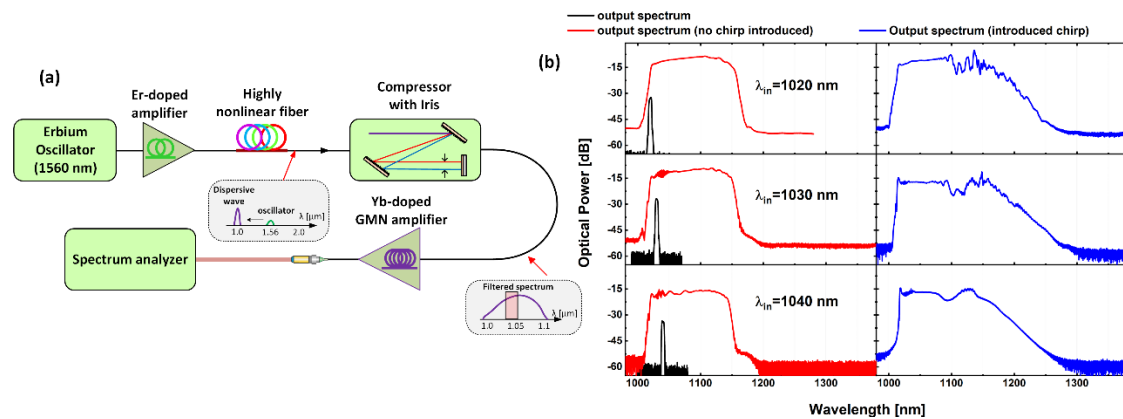


Fig. 1 (a) a simplified schematic of the experimental system; (b) selected optical spectra recorded for the input pulse and for the output pulse with the input pulse compressed and stretched.

By examining the output spectra of the amplifier, we detect a significant reliance of its response on the input parameters. Compressed pulses across each band result in spectra of comparable width, yet a length of 1020 ensures the minimal distortion of the output pulse spectrum. In contrast, for uncompressed pulses, an increase in the input pulse wavelength results in the spectrum becoming "smooth".

Funding: The research was fully funded by the National Science Center (NCN) under grant no. 2021/42/E/ST7/00111.

References

- [1] N. Nishizawa, Jpn. J. Appl. Phys.53, , 090101 (2014)
- [2] M. E. Fermann and I. Hartl, Nat. Photonics 7, 868–874 (2013)
- [3] P. Sidorenko, W. Fu, and F. Wise, Optica 6,1328–1333 (2019).

Dual Beam Laser Sintering – closed loop PA12 reuse

Aleksander Kubeczek^{1,*}, Michal Olejarczyk¹, Piotr Gruber¹, Arkadiusz Antończak¹

1. Wrocław University of Science and Technology, Wybrzeże Wyspiańskiego 27, 50-370 Wrocław, Poland

Corresponding author: *aleksander.kubeczek@pwr.edu.pl

Powder Bed Fusion (PBF) is an Additive Manufacturing method that uses a laser to sinter polymer powders, commonly polyamide 12 (PA12). A major limitation of the process is thermal degradation of the feedstock due to continuous preheating, which restricts material reuse. Typically, only ~10% of the powder is effectively used [1]; the rest requires blending with virgin material or processing to restore its properties [2–6].

This study demonstrates **closed-loop reuse** of PA2201 (EOS, Krailling, Germany) using Dual Beam Laser Sintering (DBLS) [7–10], which employs two lasers – one for heating and one for sintering – eliminating the need for heaters/halogen lamps and enabling room-temperature operation. Four build iterations were conducted: the first with virgin powder, and subsequent ones with powder recycled from previous builds.

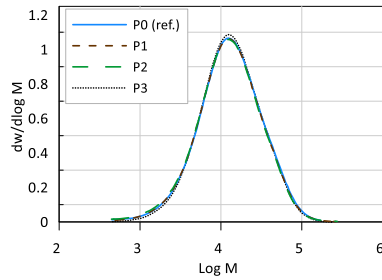


Fig. 1. Curves of the differential function of molecular mass distribution MWD for PA12 virgin and postprocess powders.

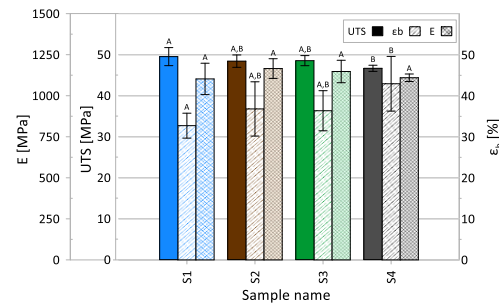


Fig. 2. Mechanical properties of PA12 tensile specimens.

Tab. 1. MVR index of PA12 virgin and postprocess powders.

Powder	P0 (ref.)	P1	P2	P3
MVR [cm ³ /10 min]	29.64 ± 2.10	32.09 ± 2.66	31.51 ± 1.56	31.04 ± 4.13

Analysis showed minimal degradation across reuse cycles. Gel permeation chromatography and melt viscosity tests revealed stable molecular weight distribution (Fig. 1, Tab. 1), while tensile testing confirmed consistent mechanical performance (Fig. 2). Minor changes in powder flow and particle morphology were observed, likely due to SiO₂ filler content variations, confirmed via EDS and SEM. Importantly, all reused material produced parts with mechanical properties within acceptable ranges, supporting the feasibility of **true closed-loop reuse**. These findings highlight DBLS as a promising alternative for sustainable and efficient PBF manufacturing.

Overall, DBLS enabled effective reuse of PA12 without significant loss in material quality. Further development involving galvanometric scanning is underway to enhance precision and further reduce degradation.

Funding and acknowledgements.

This research was supported by a pro-quality subsidy granted by the Faculty of Mechanical Engineering at the Wrocław University of Science and Technology (Poland) with funding from the “Excellence Initiative – Research University” program for 2024, the task “Reducing thermal degradation of polyamide 12 using dual beam laser sintering process” and the Opus project “Laser modification of bioresorbable polymeric materials in thermal processes of additive manufacturing” financed by the National Centre of Science (UMO-2017/27/B/ST8/01780).

References

- [1] S. Dadbakhsh, L. Verbelen, O. Verkinderen, D. Strobbe, P. Van Puyvelde, and J.-P. Kruth, “Effect of PA12 powder reuse on coalescence behaviour and microstructure of SLS parts,” *European Polymer Journal*, vol. 92, pp. 250–262, Jul. 2017, doi: 10.1016/j.eurpolymj.2017.05.014.
- [2] K. Dotchev and W. Yusoff, “Recycling of polyamide 12 based powders in the laser sintering process,” *Rapid Prototyping Journal*, vol. 15, no. 3, pp. 192–203, Jan. 2009, doi: 10.1108/13552540910960299.
- [3] S. Weinmann and C. Bonten, “Recycling of PA12 powder for selective laser sintering,” *AIP Conference Proceedings*, vol. 2289, no. 1, p. 020056, Nov. 2020, doi: 10.1063/5.0029945.
- [4] Y. Chen, H. Zhang, S. Majumdar, R. A. T. M. van Benthem, J. P. A. Heuts, and R. P. Sijbesma, “Dynamic Polyamide Networks via Amide–Imide Exchange,” *Macromolecules*, vol. 54, no. 20, pp. 9703–9711, Oct. 2021, doi: 10.1021/acs.macromol.1c01389.
- [5] M. Olejarczyk et al., “New powder reuse schema in laser-based powder bed fusion of polymers,” *Waste Management*, vol. 187, pp. 11–21, Oct. 2024, doi: 10.1016/j.wasman.2024.06.030.
- [6] L. Wang, A. Kiziltas, D. F. Mielewski, E. C. Lee, and D. J. Gardner, “Closed-loop recycling of polyamide12 powder from selective laser sintering into sustainable composites,” *Journal of Cleaner Production*, vol. 195, pp. 765–772, Sep. 2018, doi: 10.1016/j.jclepro.2018.05.235.
- [7] P. Gruber, A. Kubeczek, M. Olejarczyk, G. Ziółkowski, and A. J. Antończak, “Laser sintering of polyamide 12 with limited thermal degradation,” *Journal of Manufacturing Processes*, vol. 124, pp. 834–842, Aug. 2024, doi: 10.1016/j.jmapro.2024.06.056.
- [8] A. J. Antończak et al., “First, do not degrade – Dual Beam Laser Sintering of polymers,” *Additive Manufacturing*, vol. 53, p. 102715, May 2022, doi: 10.1016/j.addma.2022.102715.
- [9] B. Kryszak et al., “Mechanical properties and degradation of laser sintered structures of PLA microspheres obtained by dual beam laser sintering method,” *Int J Adv Manuf Technol*, vol. 120, no. 11, pp. 7855–7872, Jun. 2022, doi: 10.1007/s00170-022-09253-6.
- [10] P. Gruber et al., “High porosity composite structures produced from poly(lactic acid)/hydroxyapatite microspheres using novel Dual Beam Laser Sintering method: Analysis of structural, mechanical and thermal properties,” *Journal of Manufacturing Processes*, vol. 84, pp. 1284–1297, Dec. 2022, doi: 10.1016/j.jmapro.2022.11.010.

Methods for generating few-cycle laser pulses in the near- and mid-infrared spectral bands

Michał Pietrzak*, Jakub Jaworski, Arkadiusz Hudzikowski,
Aleksander Gluszek, Jarosław Sotor, Maciej Kowalczyk

Faculty of Electronics, Photonics and Microsystems,
Wrocław University of Science and Technology, Wybrzeże Wyspiańskiego 27, 50-370 Wrocław, Poland

Corresponding author: *michal.pietrzak@pwr.edu.pl

Ultrashort laser pulses in the femtosecond regime (10^{-15} s) play a crucial role in scientific research such as light-matter interactions, but also in fields like medicine and material processing. Several applications strongly benefit from high instantaneous power, and thus require compression of laser pulses to few-cycle durations. Due to the Fourier transform relationship between pulse duration and spectral width [1], shortening a laser pulse in time necessitates spectral broadening, which often has to be followed by temporal compression [2].

In this work, we present two methods for spectral broadening based on self-phase modulation (SPM) implemented in two different laser systems operating in the near-infrared (NIR) and mid-infrared (MIR) spectral bands. The NIR source is a commercial ytterbium-based fiber laser amplifier emitting 307 fs pulses at 1030 nm, with an energy of 116 μ J per pulse (Trumpf). Spectral broadening for this source is performed in a gas-filled multi-pass cell (MPC) using xenon at a pressure of 3.0 bar. The MIR laser source is a Cr:ZnS-based solid-state laser operating at a central wavelength of 2300 nm, producing 30 fs pulses with an energy of 25 nJ [3]. In this case, spectral broadening is achieved using a single pass through a bulk plate made of titanium dioxide (TiO₂). Fig. 1 presents the setups for NIR (a) and MIR (b) laser sources together with the optical spectra measured pre- and post-SPM.

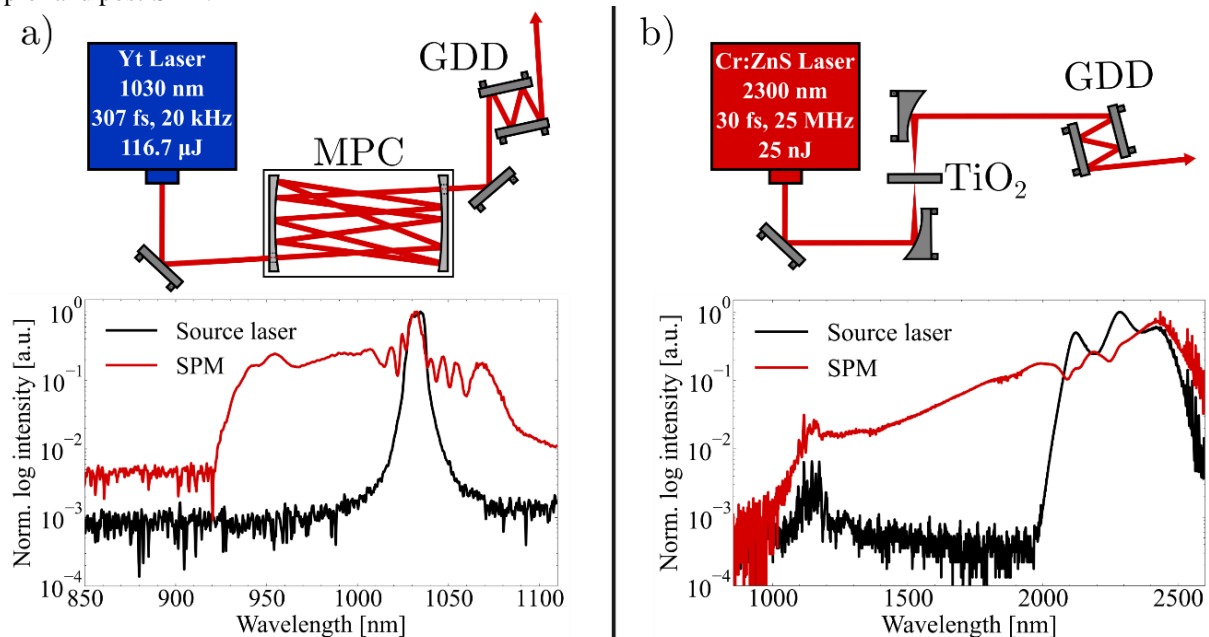


Fig. 1. Experimental setups for the NIR and MIR sources with the corresponding output spectra before and after spectral broadening: (a) NIR setup: Yb: fiber laser with spectral broadening in a xenon-filled multi-pass cell; (b) MIR setup: Cr:ZnS laser with spectral broadening in a TiO₂ bulk plate.

Subsequently, temporal compression is required to shorten the pulses to reach few-cycle durations. In case of both laser systems, this is achieved using dispersive mirrors, which introduce negative group delay dispersion (GDD) to counteract the dispersion accumulated during spectral broadening process. In the case of the NIR system, pulse durations below 30 fs are achieved, while the MIR system reaches durations below 10 fs.

Funding and acknowledgements: NAWA (BPN/PPO/2022/1/00028); Max Planck Partner Group Programme; The project “Ultrastable pulsed lasers covering the spectral range from near to far infrared” (FENG.02.02-IP.05-0069/23) is carried out within the First Team programme of the Foundation for Polish Science co-financed by the European Union under the European Funds for Smart Economy 2021-2027 (FENG).

References

- [1] U. Keller, *Ultrafast Lasers: A Comprehensive Introduction to Fundamental Principles with Practical Applications* (Springer International Publishing, Cham, 2021).
- [2] T. Nagy, S. L. Peter, and L. Veisz, “High-energy few-cycle pulses: post-compression techniques,” *Adv. Phys. X* **6**, 1845795 (2021).
- [3] M. Kowalczyk *et al.*, “Ultra-CEP-stable single-cycle pulses at 2.2 μ m,” *Optica* **10**, 801–811 (2023).

Depolarization of Raman Solitons in Birefringent Photonic Crystal Fibers: Mechanisms and Modeling

Rafał Cichowski^{1,*}, Karolina Stefańska^{1,2}, Paweł Mergo^{2,*}, Tadeusz Martynkien¹, Karol Tarnowski¹

1. Department of Optics and Photonics, Wrocław University of Science and Technology, Wybrzeże Wyspiańskiego 27, 50-370 Wrocław, Poland

2. DIET, Sapienza Università di Roma, via Eudossiana 18, 00184 Rome, Italy

3. Laboratory of Optical Fiber Technology, Maria Curie-Skłodowska University, Pl. M. Curie-Skłodowskiej 3, 20-031 Lublin, Poland

Corresponding author: *rafal.cichowski@pwr.edu.pl

Raman solitons are intense, ultrashort optical pulses that experience a self-frequency shift when propagating through optical fibers operating in the anomalous dispersion regime. These solitons are widely used in the development of spectrally tunable light sources based on fiber lasers and optical fibers, with their spectral position controllable via pump laser power. When birefringent fibers are employed, the generated light typically exhibits high polarization purity [1]. However, certain depolarization mechanisms—namely linear polarization coupling, nonlinear polarization coupling, and orthogonal Raman scattering—can degrade this purity under specific conditions [2].

In this work, we present a numerical model based on a system of coupled nonlinear Schrödinger equations that incorporates these polarization effects. We also experimentally characterize the soliton generation and polarization purity in two types of birefringent photonic crystal fibers. By comparing numerical simulations with experimental measurements, we validate the accuracy of the model. Furthermore, the simulations provide additional insight into the nonlinear dynamics through spectrogram analysis.

Funding and acknowledgements. The presented results were achieved within project supported by The National Science Center, Poland (2018/30/E/ST7/00862).

References

- [1] O. Szewczyk, P. Pala, K. L. Tarnowski, J. Olszewski, C. Lu, A. Foltynowicz, F. Senna Vieira, P. Mergo, J. Sotor, G. Sobon, and T. Martynkien, Dual-wavelength pumped highly birefringent microstructured silica fiber for widely tunable soliton self-frequency shift, *IEEE Journal of Lightwave Technology*, 39(10), 3260-3268 (2021), DOI: 10.1109/JLT.2021.3057657
- [2] K. Stefańska, S. Majchrowska, K. Gemza, G. Soboń, J. Sotor, P. Mergo, K. Tarnowski, and T. Martynkien, Soliton trapping and orthogonal Raman scattering in a birefringent photonic crystal fiber, *Optics Letters*, 47(16), 4183-4186 (2022), DOI: 10.1364/OL.463643

Design and simulation of a side-pump fiber combiner for high-power lasers and amplifiers

Szymon Matczak^{1,*}, Dorota Stachowiak¹, Grzegorz Sobóń¹

1. Wrocław University of Science and Technology, Wybrzeże Wyspiańskiego 27, 50-370 Wrocław, Poland

Corresponding author: *szymon.matczak@pwr.edu.pl

The dynamic growth of photonic sciences requires the development of innovative technologies for fabricating non-standard fiber optic components, which are crucial for the evolution of modern lasers, light sources, etc. An excellent example of such a component is a power combiner [1]. The most commonly used type of power combiner is based on a tapered fused bundle (TFB) configuration [1]. During its fabrication, several multi-mode pumping fibers are placed around a single-mode signal fiber, forming an input fiber bundle in which the signal fiber is placed in the center. Then, the fiber bundle is fused and tapered down, cleaved, and spliced to the output double-clad (DC) fiber [2]. Usually, a high taper ratio of the fiber bundle is required, which is problematic for polarization-maintaining (PM) signal fibers. Typically, a PM fiber has stress rods that introduce strong birefringence. Tapering a PM fiber with such a high taper ratio causes additional stress inside the fiber and expansion of the mode field along the axis of the rods, resulting in an elliptical beam shape and thus increasing signal transmission losses.

In this work, we present our research on a side-pumping combiner scheme, which might be beneficial for PM signal fibers, because the fabrication process has minimal impact on the PM fiber: it is not cleaved or spliced, and the input fiber is simultaneously the output fiber. The design involves the coreless passive fiber (CPF) as a pump fiber (FUD-3582, MM-125-FA, Coherent) being bent around the DC fiber (SM-GDF-1550, Coherent). To analyze the optical properties of the designed combiner, numerical simulations were performed using the RsoftCAD BeamPROP software based on the Beam Propagation Method (BPM). The simplified model shown in Fig. 1 consists of two components: a tapered CPF, which delivers the pump light, and a signal DC fiber, into which the pump light is coupled.

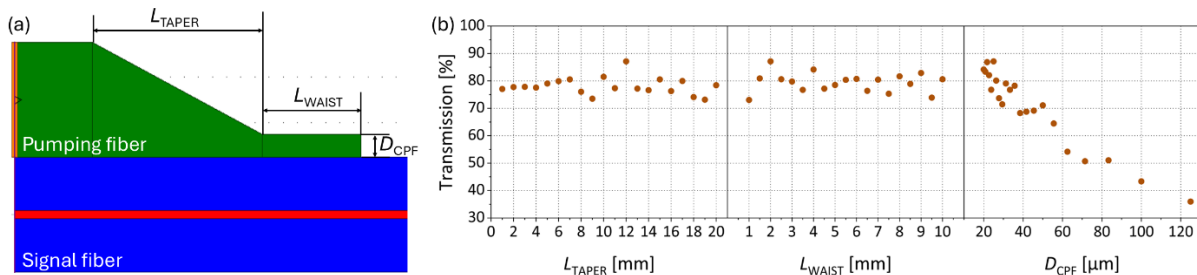


Fig. 1 (a) Simplified model designed in the BeamPROP software detailing the variable geometric parameters of the structure, (b) Simulations of transmission as a function of taper length (L_{TAPER}), length of tapered waist (L_{WAIST}), waist diameter (D_{CPF}).

The geometry of the coupler was defined by three parameters: the taper length (L_{TAPER}), the tapered waist length (L_{WAIST}), and the CPF diameter at the waist section (D_{CPF}). The simulations aimed to investigate the influence of these variables on the pump radiation coupling efficiency from the pump fiber to the inner clad of the signal DC fiber. The results, presented in Fig. 1 (b), show that both L_{TAPER} and L_{WAIST} have a relatively minor effect on coupling efficiency, with transmission levels maintained between 80% and 90%. Respectively, maximum values were achieved for the $L_{TAPER} = 12$ mm and $L_{WAIST} = 2$ mm. In contrast, the parameter D_{CPF} seems to be more critical. The transmission reaches a maximum for the diameter range of 30 – 40 μm and drops for bigger diameters, increasing propagation losses. Based on the simulation results, an optimal set of geometric parameters can be identified, ensuring efficient power coupling between the fibers. This will allow us to fabricate such a structure using the Large Diameter Splicing (LDS) system, as it has proven its usefulness in the tapering and fabrication of fiber optic structures [2,3].

Funding and acknowledgements. The work was supported by the project Minigrants for doctoral students of the Wrocław University of Science and Technology, LIDER (LIDER14/0070/2023) of the National Centre of Research and Development, and Preludium BIS (2021/43/O/ST7/00757) of the National Science Centre (NCN).

References

- [1] D. Stachowiak, “High-Power Passive Fiber Components for All-Fiber Lasers and Amplifiers Application—Design and Fabrication”. *Photonics* 5, 38 (2018).
- [2] D. Stachowiak, et al., “ $(5 + 1) \times 1$ pump and signal power combiner with 9/80 μm feed-through signal fiber”. *Opt. Laser Technol.* 93, 33–40 (2017).
- [3] S. Matczak, et al., “Design and fabrication of fiber optic microlenses using an arc fusion splicing system”. *J. Light. Technol.* doi: 10.1109/JLT.2025.3563232 (2025).

Controllable optical fibre coupler with liquid crystal cladding

A.Merchel^{1,*}, K.Stasiewicz¹

1. *Institute of Applied Physics, Military University of Technology, gen. Sylwestra Kaliskiego 2, 00-908, Warsaw, Poland* * Corresponding author: aleksandra.merchel@student.wat.edu.pl

The development of optical fibre sensors stands as a testament to the relentless pursuit of innovation in sensing technologies. From their humble beginnings as a niche concept to their current status as indispensable tools across diverse industries, optical fibre sensors have evolved remarkably. However, we are still looking for a new solution that can affect light propagation in an optical path of sensor arrangements. Many measuring systems use couplers to split the beam into several tracks. Couplers are characterized by a constant division of the distributed power for a given wavelength. In the proposed work, we focused on creating a tunable coupler in the selected range using additional materials controlled by an electric field.

Many works are connected with placing the coupler in the liquid crystal, but such an approach causes a change in both arms. In our works, we focus on the influence of only the change of power in a coupled arm. The tunable coupler's construction consists of simultaneously making two tapered optical fibres with a diameter of about $10\mu\text{m}$ at a mutual distance of not more than $3\mu\text{m}$ (ensuring that they remain sufficiently close without physical contact) and placing it in a liquid crystal cell with LC 6CHBT. The structure of the liquid crystalline cell is based on two planar plates covered by an ITO conductive layer, which allows an electric field to be applied, and a rubbing layer, designed to prearrange the LC molecules. This configuration alters the refractive index of the liquid crystal and thus the parameters and light propagation along the optical path of tapered optical fibers immersed in it. Altering the refractive index provides precise control over the beam transition between the main and coupled arms. The constructed system empowers the manipulation of power in the receiving arm, and thanks to the applied voltage, it is possible to change the propagated power.

The article shows the first experimental study on constructing the presented coupler for selected wavelengths using multimode optical fibers and liquid crystal named 6CHBT. The LC cell with tapers was steering with a voltage from 0-200V. Additionally, the electric field was modulated with a frequency of 1-10Hz to observe the possibility of fast tuning of the division ratio in a new coupler. Fig. 1 presents the results of the obtained coupler. As can be seen, the power in a main arm is almost constant, and for a coupled arm, power can be controlled by the change of electric field and connected with it change LC molecules orientation – change of the refractive index.

The first results show that it is possible to create a new tunable coupler by setting the appropriate technological parameters, including the distance between tapers, their diameter, and the type of liquid crystal that will surround them.

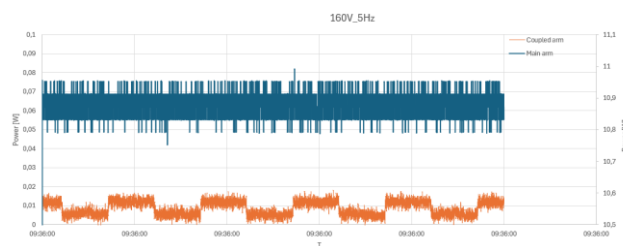


Fig. 1 Results for 160V, 5Hz

Doped fiber amplifiers in laser spectroscopy of methane: performance, benefits and effects on signal quality

Magdalena Zatorska¹, Michał Nikodem¹, Grzegorz Gomółka²

1. Department of Optics and Photonics, Wrocław University of Science and Technology, Wybrzeże Wyspińskiego 27, 50-370 Wrocław, Poland

2. Department of Field Theory, Electronic Circuits and Optoelectronics, Wrocław University of Science and Technology, Wybrzeże Wyspińskiego 27, 50-370 Wrocław, Poland

Corresponding author: magdalena.zatorska@pwr.edu.pl

Laser spectroscopy in the near-infrared (NIR) region is a powerful technique for gas sensing due to its high sensitivity, selectivity, and compatibility with compact, cost-effective fiber-optic systems. While the NIR region does not cover fundamental molecular transitions found in the mid-infrared, it still enables low detection limits for gases such as methane and carbon dioxide. A key advantage of NIR systems is the ability to integrate optical amplifiers, which can significantly enhance performance. In methods such as photoacoustic spectroscopy (PAS), higher optical power directly improves the signal-to-noise ratio. Various doped fiber amplifiers: erbium, bismuth, thulium, as well as Raman and semiconductor amplifiers, have been applied in PAS and remote sensing systems [1-3]. Most previous studies focus on signal enhancement, while the potential drawbacks, such as baseline distortion or signal shape alteration, are less often addressed.

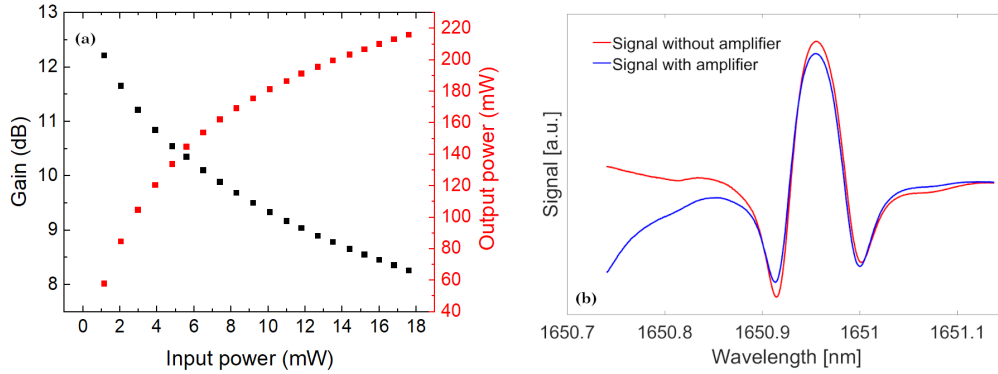


Fig. 1: (a) Gain (black, left axis) and output power (red, right axis) of the bismuth-doped fiber amplifier (BDFFA) measured at 1651 nm as a function of input optical power. (b) Wavelength Modulation Spectroscopy (WMS) signals of methane measured with and without BDFFA. The amplified signal (blue) shows a slight baseline offset due to amplifier-induced distortion, while the peak shape and amplitude remain largely preserved.

In this work, we evaluate the performance and influence of bismuth- and thulium-doped fiber amplifiers in several laser-based methane sensing techniques: Wavelength Modulation Spectroscopy (WMS), Quartz-Enhanced Photoacoustic Spectroscopy (QEPAS), and Phase-Sensitive Spectroscopy - a novel method inherently immune to source power fluctuations. For WMS and QEPAS, the nonlinear response of the amplifiers introduces a background signal, which may affect measurement accuracy despite minimal impact on signal symmetry or peak height. In contrast, PSS maintains consistent signal shape with or without amplification, demonstrating its robustness to power-related distortions.

References

- [1] G. Gomółka, A. M. Khegai, S. V. Alyshev, A. S. Lobanov, S. V. Firstov, and M. Nikodem, "Characterization of a single-frequency bismuth-doped fiber power amplifier with a continuous wave and modulated seed source at 1687 nm", *Appl. Opt.* 59, 1558–1563 (2020).
- [2] J. Aubrecht, J. Pokorný, B. Švejkarová, M. Kamrádek, and P. Peterka, "Broadband thulium fiber amplifier for spectral region located beyond the L-band", *Opt. Express* 32, 17932–17941 (2024).
- [3] R. Bauer, T. Legg, D. Mitchell, G. M. H. Flockhart, G. Stewart, W. Johnstone, and M. Lengden, "Miniaturized photoacoustic trace gas sensing using a Raman fiber amplifier", *J. Lightwave Technol.* 33, 3773–3780 (2015).

Comparing the optical properties of ZBLAN fibers produced using an experimental compact draw tower and a standard draw tower

Andrija Djordjevic^{1,2,3,*}, Grzegorz Stepniewski⁴, Piotr Bienias^{4,5}, M. Ali Arat³, Hubert Moser³, Ka S. Wu⁶, Ehab Salih⁶, Heike Ebendorff-Heidepriem⁶, Ryszard Buczynski^{2,4}, Stephan Leyer¹

1. Faculty of Science, Technology and Medicine, University of Luxembourg, 4365 Luxembourg, Luxembourg

2. Faculty of Physics, University of Warsaw, 02-093 Warsaw, Poland

3. Flawless Photonics S.à r.l., 2714 Luxembourg

4. Lukaszewicz Research Network – Institute of Microelectronics and Photonics, 02-668 Warsaw, Poland

5. Faculty of Physics, Warsaw University of Technology, 00-662 Warsaw, Poland

6. Institute for Photonics and Advanced Sensing, University of Adelaide, Adelaide, SA 5005, Australia

Corresponding author: *a.djordjevic@uw.edu.pl

ZBLAN optical fibers produced in microgravity have shown greater quality according to NASA research conducted in the 1990s [1-3]. To be able to use this advantageous environment, Flawless Photonics built an automated compact draw tower, fitting in the microgravity science glovebox aboard the International Space Station. This machine was tested on ground by producing ZBLAN fibers. The multimode fiber drawn during one of these tests, is compared to a ZBLAN fiber produced by a conventional draw tower. The properties compared are the numerical aperture, the attenuation, the concentricity of the core in the clad, and the circularity of the core.

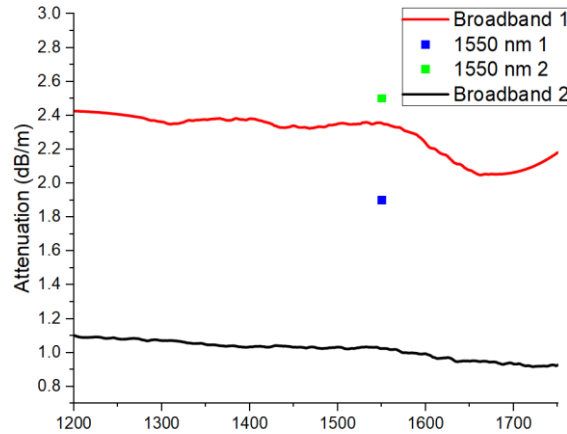


Fig. 1 Attenuation of experimental and standard production fiber

Table 1. Physical properties: compact vs. standard draw tower

	Compact draw tower	Standard draw tower
Height (cm)	51	420
Depth (cm)	40	100
Width (cm)	81	120
Volume (m3)	0.15	5.04
Weight (kg)	62	2300

Funding and acknowledgements. This work was supported in part by the Luxembourg National Research Fund under the Industrial Fellowship Grant, by the European Space Agency under the LuxImpulse program of the Luxembourg Space Agency, and by H2020 PhotonHub Europe No. 101016665. This work was performed in part at the OptoFab node of the Australian National Fabrication Facility utilizing Commonwealth and SA State Government funding.

References

- [1] G. U. Y. A. Smith, S. E. Kosten, and G. L. Workman, 'Materials processing apparatus development for fluoride glass', 1994.
- [2] G. L. Workman, G. U. Y. A. Smith, and S. E. Kosten, 'Phase A design study of microgravity fluoride fiber puller', 1994.
- [3] G. L. Workman, G. U. Y. A. Smith, S. O'Brien, and L. Adcock, 'ZBLAN Microgravity Study', 1995.

GROMiT – Galinstan Rotating Mirror Telescope with an Off-Zenith Observation System

Piotr Maruszak^{1*}, Ignacy Stencel¹, Gabriela Przybyła^{1,2},
Paweł Rukat¹, Weronika Seroczyńska², Andrzej Stach¹
Filip Łabaj³, Anna Pakuła¹

1. Faculty of Mechatronics, Warsaw University of Technology, ul. św. Andrzeja Boboli, 02-525 Warszawa, Poland

2. Faculty of Materials Engineering, Warsaw University of Technology, ul. Woloska 141, 02-507 Warszawa, Poland

3. Faculty of Electronics and Information Technology, ul. Nowowiejska 15/19, 00-665 Warszawa, Poland

Corresponding author: * piotr.maruszak419@gmail.com

We have designed, constructed, and are currently in the process of testing a miniature, Galinstan (Ga, In and Sn alloy) liquid mirror-based telescope system. The design is based on the documented work of R. W. Wood [1] and E. F. Borra [2], however, we have scaled the telescope down, made it portable and used Galinstan instead of mercury as a mirror material.

The core part of the designed telescope system is a rotational main mirror, which optical surface is created by rotating a 3D printed mirror container. For our design constraints of mirror diameter 250 mm and focal length between 1200 and 2000 mm, the required rotational frequency is between 0.20 Hz and 0.35 Hz. The main mirror is rotated by using a BLDC motor with Hall-sensor based PID speed control, coupled with a planetary gear module and a belt transmission to achieve the required frequencies while avoiding vibrations.

The secondary mirror is motorized, allowing the operator to change the optical path. On the top of the system, a motorized, directional mirror provides the ability to view off-zenith objects up to 30° above the horizon without losing any light falling onto main mirror. The acquisition of images is performed using a dedicated CMOS camera (ZWO ASI 533 MC-P).

Several measurements of the constructed system will be performed, testing its angular resolution, light power and field-of-view.

Funding and acknowledgements.

The project is funded by Warsaw University of Technology through the Rector's Grant for Student Research Clubs (2024).

References

- [1] R. W. Wood. "The Mercury Paraboloid as a Reflecting Telescope". *Astrophysical Journal*, vol. 29, March 1909.
- [2] E. F. Borra. "The liquid-mirror telescope as a viable astronomical tool". *Journal of the Royal Astronomical Society of Canada*, vol. 76; August 1982.

Construction of a laboratory model of an adaptive optics module for an amateur telescope

Pawel Rukat

Warsaw University of Technology, Plac Politechniki 1, 00-661 Warsaw, Poland
pawel.rukat.stud@pw.edu.pl

The work is based on the use of a mathematical model describing the perturbations of an optical medium such as the Earth's atmosphere to simulate the possibility of wavefront shape correction in an amateur astronomical telescope (with an aperture ranging between 0,15 m to 0,5 m) in order to improve the resolving power of the instrument bringing it closer to the diffraction limited performance.

Both theoretical and empirically fitted models show the dependence of the atmospheric scintillation coefficient on the wavelength and height of the observations made through the coherence length parameter [1]. The implementation of one of these models in the Matlab environment allows the generation of a wavefront phase structure function in the aperture plane and thus allows the quantitative and qualitative analysis of the possibility of its correction (restoration of flat shape) by simulating the operation of a Shack-Hartmann measurement sensor and segmented adaptive mirror with one (tip) and three degrees of freedom (tip-tilt).

The developed simulation model enables quantitative analysis of the quality of wavefront shape correction depending on the number of sensor measurement points (number of sub-apertures in the microlens array) and the number of segments of the adaptive mirror.

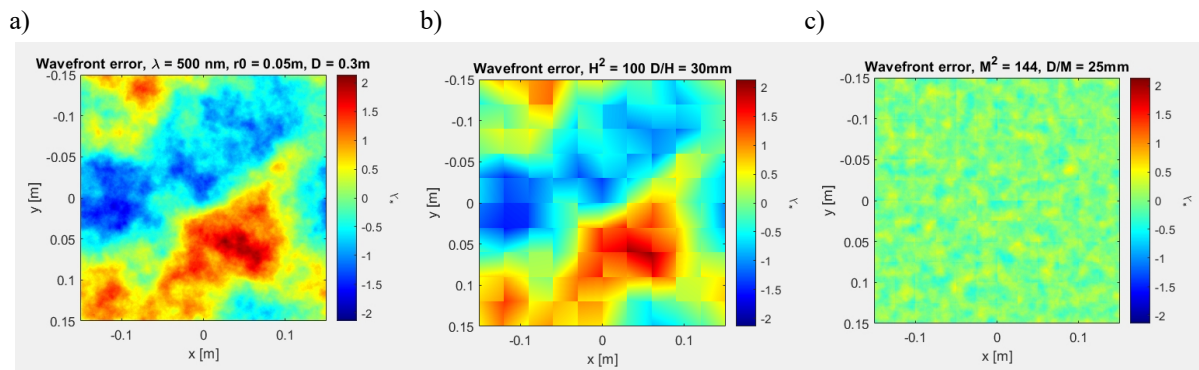


Fig. 1 An example iteration of the phase structure function of a turbulent wavefront (a) for a 30 cm aperture telescope operating in visible light under degraded atmospheric conditions (with a coherence length r_0 of 5 cm). The Shack-Hartmann measurement simulation (b) using local gradients of the phase structure function, and a simulation of a three-degree-of-freedom correction algorithm (c) for a segmented tip-tilt mirror provides a promising results indicating that turbulent wavefront propagating through a small aperture telescope can be corrected by a potential adaptive mirror module.

The above results, obtained for 100 sensor measurement points (H^2) and 144 mirror segments (M^2), indicate that proper wavefront shape correction is feasible, leading to a significant improvement in the resolving power of the instrument operating under reduced coherence length conditions.

Table 1. Example results obtained for an output wavefront with given input parameters.

$\lambda = 500 \text{ nm}$ $r_0 = 0,05 \text{ m}$ $D = 0,3 \text{ m}$ $H^2 = 100$ $M^2 = 144$	Passive optics	Adaptive segmented mirror with 1 degree of freedom (tip)	Adaptive segmented mirror with 3 degrees of freedom (tip-tilt)	Diffraction limited optics
RMS wavefront error	$\lambda/1,25$	$\lambda/4,25$	$\lambda/7,34$	0
Strehl's ratio	0,043	0,133	0,479	1
Resolving power	2,03"	1,15"	0,61"	0,42"

The results obtained made it possible to create the first model of a potential prototype adaptive mirror module and to develop a laboratory method for measuring the quality of wavefront correction. The above research is an important milestone on the path of promoting advanced optical technologies in the amateur instrument market.

References

[1] Hardy J. W., 1998, Adaptive optics for astronomical telescopes, Oxford University Press, Oxford.

Laser-base gas sensing – using neural networks to speed-up and simplify data analysis

Przemysław Chmielowski^{1,*}, Michał Nikodem¹

1. Wrocław University of Science and Technology, Wybrzeże Wyspiańskiego 27, 50-370 Wrocław, Poland

Corresponding author: *Przemyslaw.chmielowski@pwr.edu.pl

Optical spectroscopy is a powerful tool in gas sensing applications. Laser-based spectroscopy offers high sensitivity and selectivity. Additional advantages include fast response time, compact design, and no need for sample preparation. Moreover, some optical gas sensors can operate continuously in real-world, non-laboratory conditions with only minimal maintenance.

In theory, optical gas sensing is relatively straightforward: a tunable laser source and a detector are used to record an optical spectrum. By analyzing the recorded absorption lines, one can retrieve molecular concentration information (as shown in Fig. 1). In practice, however, the analysis becomes challenging due to additional signal components, such as fluctuating, nonlinear baselines and unwanted interference fringes which are superimposed on the absorption features. Advanced algorithms capable of extracting molecular concentrations through full-spectrum fitting, including modelling of background signals, can take several seconds to process a single spectrum (or even tens of seconds for complex spectra). This becomes impractical when working with high-speed data acquisition.

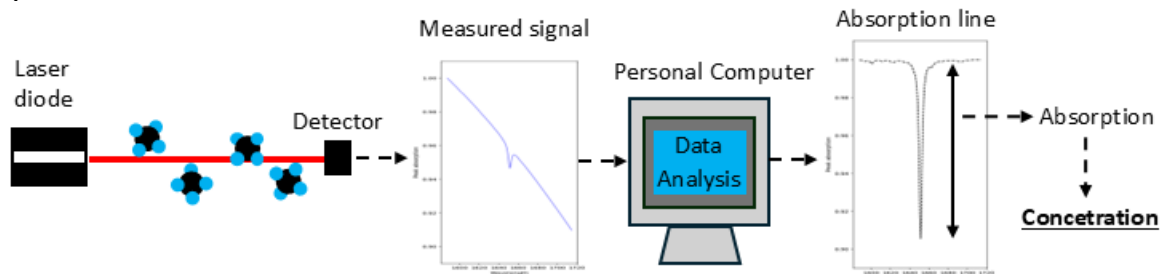


Fig. 1. Schematic diagram of a tunable diode laser absorption spectrometer: laser diode and detector are used to record optical spectrum; recorded signal is analyzed in order to remove unwanted signals (such as baseline or optical fringes) and retrieve information about molecular concentration.

In our work, we investigate whether neural network (NN)-based algorithms can be used for rapid spectral analysis. Our initial experiments are focused on using NN to remove fluctuating baseline from absorption spectra recorded with tunable diode laser absorption spectroscopy (TDLAS). Few examples are demonstrated in Fig. 2 where we show input signals, expected/desired signals and absorption line profiles predicted using NN-based algorithm.

Preliminary results show that while NNs are significantly faster than traditional fitting methods, they can also introduce unexpected errors. This is visible in Fig. 2: while NN usually correctly retrieves the absorption line profile (a-d) in some cases prediction is significantly off (e). During my presentation, I will highlight critical aspects of NN training that significantly affect the final performance of this approach.

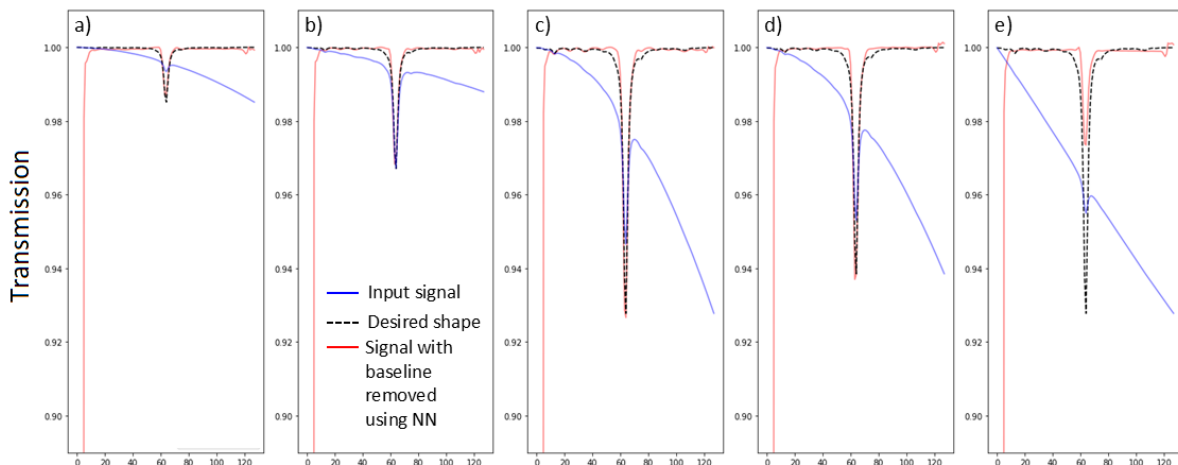


Fig. 2. Examples of absorption line retrieval from signals recorded using the TDLAS method. Plots a-d show that the NN-based algorithm can accurately predict the absorption line shape. However, in some cases (e.g., plot e), the prediction is significantly off.

Adaptive spiral phase plates for generation of optical vortices

Tomasz Jankowski^{1*}, Noureddine Bennis¹, Anna Pakuła², Przemysław Morawiak¹,
Jose Francisco Algorri³

1. Faculty of Advanced Technologies and Chemistry, Military University of Technology, Warsaw 00-908, Poland

2. Faculty of Mechatronics, Warsaw University of Technology, 'Sw. Andrzeja Boboli 8, 02-525 Warsaw, Poland

3. Photonics Engineering Group, University of Cantabria, 39005 Santander, Spain

Corresponding author: *tomasz.jankowski@wat.edu.pl

In recent years, extensive research has focused on optical vortices and the devices that generate them, motivated by their broad applicability in areas such as beam shaping, free-space optical communication, optical tweezers, and more [1]. The core principle behind the generation of these unique wavefronts lies in imparting an azimuthal phase dependence of the form $e^{-il\phi}$, where ' l ' denotes the topological charge—representing the number of complete 2π phase rotations—and ' ϕ ' is the azimuthal angle in polar coordinates, measured in the plane perpendicular to the beam's propagation direction. When wavefronts carrying orbital angular momentum (OAM) are focused, they form characteristic ring-shaped intensity patterns rather than focal spots.

In this study, we present a novel method for generating optical vortices using an Adaptive Spiral Phase Plate (ASPP) based on a liquid crystal (LC) and a transmission electrode technique. The device operates through a specially designed ITO electrode topology that generates an electric field across the LC layer. A key feature is a circular transmission electrode that establishes a continuous voltage gradient between two electrical contacts (Fig. 1a). Supplementary slices (Fig. 1b) are symmetrically arranged to distribute the voltage towards the center of the device.

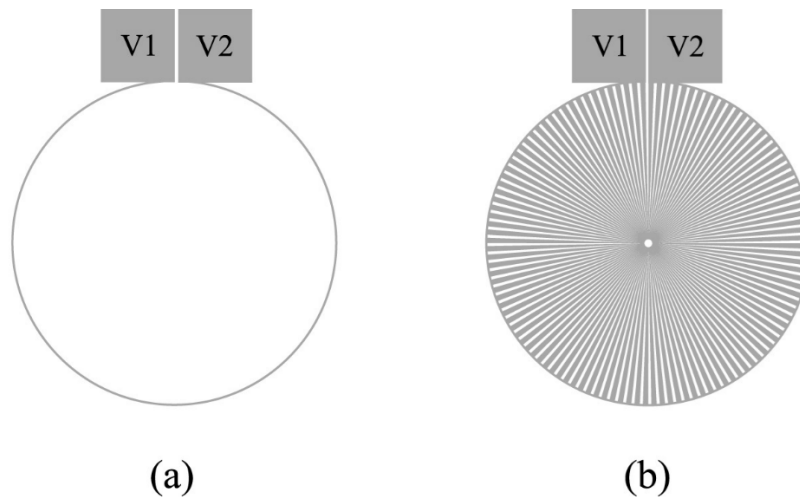


Fig. 1 (a) Schematic depiction of the circular transmission electrode alone and (b) including the ITO slices evenly arranged to distribute the voltage

Applying specific voltage configurations to the contacts enables dynamic tuning of the ASPP. Experimental validation involved simultaneous measurements of azimuthal optical phase retardation and the resulting shape of vortex beam [2]. The device allows tunability in both the magnitude and direction of the topological charge. Demonstrated results include topological charges ranging from ± 1 to ± 4 using 6CHBT liquid crystal ($\Delta n = 0.16$), with potential for higher charges using materials with greater birefringence.

Funding and acknowledgements: This work was supported by ACTPHAST 4R Innovation Project and UGB-22-725.

References

- [1] R. Chen, H. Zhou, M. Moretti, X. Wang and J. Li, "Orbital Angular Momentum Waves: Generation, Detection, and Emerging Applications," *IEEE Communications Surveys & Tutorials*, **Vol. 22**, no. 2, pp. 840-868 (2020), doi: 10.1109/COMST.2019.2952453
- [2] T. Jankowski, N. Bennis, P. Morawiak, D.C. Zografopoulos, A. Pakuła, M. Filipiak, M. Słowikowski, J.M. López-Higuera, J.F. Algorri, "Optical vortices by an adaptive spiral phase plate", *Optics & Laser Technology*, **Vol. 176**, 111029 (2024), <https://doi.org/10.1016/j.optlastec.2024.111029>.

Optimization of femtosecond fiber laser pulses with selected metaheuristic algorithms

Alicja Kwaśny*, Mikołaj Krakowski, Grzegorz Soboń

Laser and Fiber Electronics Group, Faculty of Electronics, Photonics and Microsystems, Wrocław University of Science and Technology, Wyrbrzeże S. Wyspiańskiego 27, 50-370 Wrocław, Poland

Corresponding author: *alicja.kwasny@pwr.edu.pl

Optimizing a femtosecond fiber laser for the generation of the shortest pulse is a significant challenge – due to many adjustable parameters, finding the best settings manually can take a lot of time. As we have shown in [1], optimization of femtosecond laser pulses using spectral phase modulation is possible. In this work, we compare three machine learning (ML) algorithms in optimization of ultrashort pulses: Grey Wolf Optimizer (GWO) [2], Genetic Algorithm (GA) [3], and Crow Search (CS) [4]. All three algorithms belong to the category of metaheuristic algorithms, widely used for solving engineering problems, such as the design of multipass cells [5]. They are online machine learning algorithms, which means that they learn in real time – there is no need for prior data acquisition (dataset or knowledge about the system being optimized). In our study, we compare three population-based metaheuristic algorithms based on their performance in laser pulse optimization task.

Fig. 1 shows the experimental setup, convergence curves as well as autocorrelations of optimized laser pulse for each of the algorithms. A laser pulse with a duration of approx. 700 fs was directed to a Spatial Light Modulator (SLM) which modifies the spectral phase using a suitable mask. Next, the pulse was amplified and guided to the autocorrelator for measurements. Nonlinear spectral broadening during amplification allows for obtaining a much shorter pulse at the output in comparison to the seed pulse. In the experiment, the display of SLM was divided into 20 vertical stripes, which were modulated by the algorithms. For 20 stripes, one stripe corresponds to 1.8 nm of spectral width. In each case, the population parameter in the algorithms was set to 150 as well as the initial phase mask were the same to ensure the same conditions for each of the algorithms. Time of optimization was also identical in each presented case. The cost function, that describes the quality of the laser pulse is based on full width half maximum value, and the deviation between measured pulse and its calculated fit. That way, we care about not only about the time duration of the pulse, but also its shape.

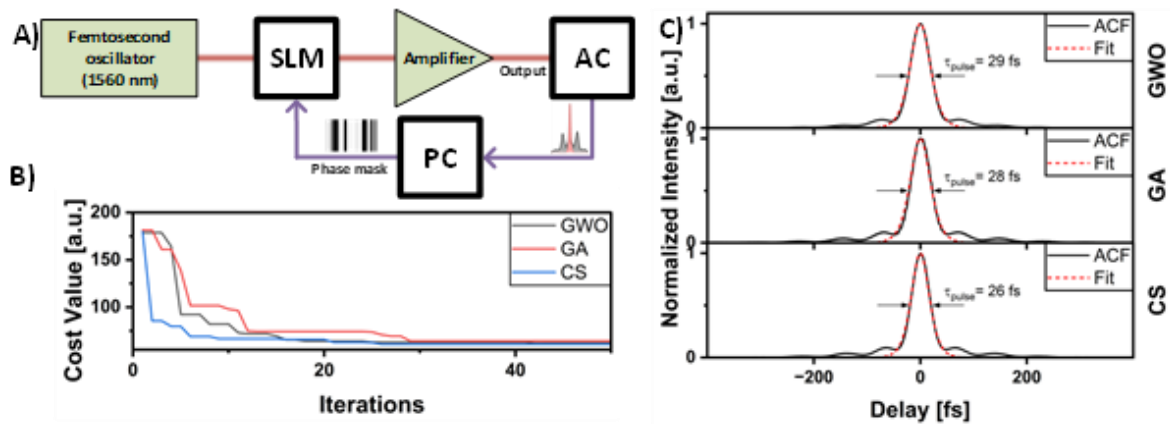


Fig. 1 A) Experimental setup. AC – Autocorrelator, PC – Personal Computer, SLM – Spatial Light Modulator B) Convergence curve, showing the value of fitness throughout iterations for tested algorithms. C) Comparison of autocorrelation function (ACF, solid black line) with sech^2 fit (Fit, dashed red line) of pulses optimized with tested algorithms.

The results show that shortening the pulse duration of the laser pulse is possible with all three presented algorithms. All of the algorithms do not require any prior training nor knowledge about structure of optimized system. However, CS algorithm found the shortest pulse (out of the three) and converged the fastest.

Funding and acknowledgements. The research was funded by National Science Centre under project no. 2021/42/E/ST7/00111.

References

- [1] M. Krakowski, A. Kwaśny, and G. Soboń, "Amplification of femtosecond pulses with AI-assisted spectral phase modulation," *Opt. Continuum* **3**, 449 (2024).
- [2] S. Mirjalili, S. M. Mirjalili, and A. Lewis, "Grey Wolf Optimizer," *Adv. Eng. Softw.* **69**, 46–61 (2014).
- [3] S. Katoch, S. S. Chauhan, and V. Kumar, "A review on genetic algorithm: past, present, and future," *Multimed Tools Appl* **80**, 8091–8126 (2021).
- [4] Q. Cheng, H. Huang, and M. Chen, "A Novel Crow Search Algorithm Based on Improved Flower Pollination," *Math. Probl. Eng.* **2021**, 1–26 (2021).
- [5] A. Hudzikowski, A. Głuszek, K. Krzempek, and J. Sotor, "Compact, spherical mirror-based dense astigmatic-like pattern multipass cell design aided by a genetic algorithm," *Opt. Express* **29**, 26127 (2021).

Temperature effect on cracking behavior of flat glass under local heating

Uliana Finaeva¹, Jan Hosek¹

1. Czech Technical University in Prague, Technicka 4, 16000 Prague, Czech Republic

Corresponding author: *uliana.finaeva@fs.cvut.cz

Understanding the behavior of glass under temperature changes is crucial for applications in optics, where optical components are often exposed to varying temperatures, high temperatures, and hot air flow. For instance, laser systems, telescope mirrors, infrared optics, and semiconductor lithography systems all involve optical elements that must withstand significant thermal stress. In aerospace, high-intensity light sources in gas lasers or optical instruments in space also experience rapid temperature shifts, making temperature management critical. These conditions can cause deformation or cracking of optical materials, affecting performance [1,2]. Knowledge of how temperature gradients influence the structural integrity of glass panes can help in designing more durable systems. We have studied how different samples of glass panes crack when exposed to hot air. We performed experiments on flat glass with one side facing hot air flow and otherwise free heat dissipation. We changed how thick the samples were to see how heat affected their cracking behaviour (time and temperature differences). We analysed how temperatures differences changed with thickness and how cracks were formed. We compared the results to existing literature data as [3,4] widening the knowledge base for new glass thicknesses. We analysed how thermocamera settings can affect acquired data and used new approach to measure glass surface temperature.

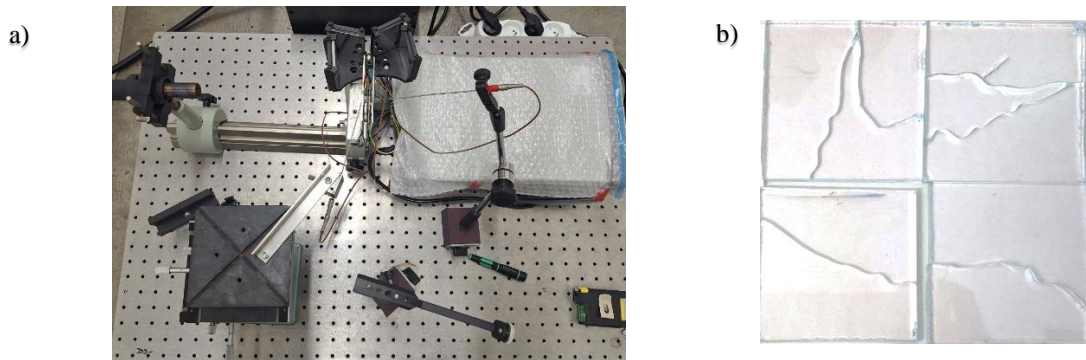


Fig. 1 (a) Experimental setup. Thermocouples are connected to the data acquisition system from both sides of the glass sample. Glass sample is set in holder with minimal stress implications. Heat gun is put to 480 degrees Celsius, and 24 l/min volume air flow is moved close to the glass when ready to perform the measurement. Temperature is simultaneously recorded on thermocamera and thermocouples until cracking of the glass. (b) Examples of resulted cracking in glass.

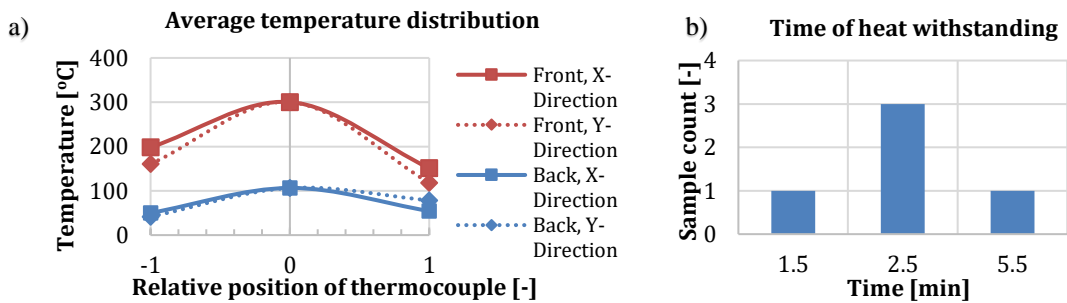


Fig. 2 Example of average data from several glass samples of specific thickness: (a) temperature achieved before destruction, (b) histogram of approximate time needed for crack to appear under the heat stress.

Funding and acknowledgements. Work has been supported by the Student Grant Competition of CTU Grant No. SGS24/124/OHK2/3T/12 “New mounting technology for glass optical elements”.

References

- [1] F. Maamar, O. Mertad, A. Mankour, “Analysis of thermo-opto-mechanical system and stress birefringence in elastically bonded optics for space applications”. *Adv. Space Res.* (2025).
- [2] T. Zhao, R. Shi, Z. Li, Y. Gao, S. Zhang, “Infrared scene projection optical system for blackbody micro cavity array”. *Infrared Phys. Technol.* 128, 104484 (2023).
- [3] Y. Yang, L. Miao, C. L. Chow, “Relative significance of temperature gradient components on cracking behavior in glass panes under thermal radiation”, *Appl. Therm. Eng.*, 131, 837-848 (2018).
- [4] Y. Wang, Q. Wang, G. Shao, H. Chen, J. Sun, L. He, K.M. Liew, “Experimental study on critical breaking stress of float glass under elevated temperature”, *Mat. Des.*, 60, 41-49 (2014).

Enhanced probing of coherent magnons with spectroscopy on higher-energy excitonic states in A-type antiferromagnet CrSBr

R.Komar¹, M.Kobecki¹, K. Mosina², A. Söll², Z. Sofer², T.Kazimierczuk¹, P.Kossacki¹

1. Faculty of Physics, University of Warsaw, Warsaw, Poland

2. Department of Inorganic Chemistry, University of Chemistry and Technology Prague, Prague, Czech Republic

Corresponding author: *rafal.komar@fuw.edu.pl

The research on 2D van der Waals magnetic materials has opened new possibilities for studying quantum phenomena in 2D materials. The magnetization in layers of such materials can allow for spin-wave (magnon) manipulation, which, if controlled correctly, could find applications in spintronics technology or magnonics research. Ideally, the magnetic ordering should coexist with the material's semiconducting character, which would significantly enhance its utility. One such promising material is CrSBr with its quasi-1D excitons and coupling of optical and magnetic properties.

CrSBr is an A-type antiferromagnet, characterized by strong ferromagnetic ordering within each layer and antiferromagnetic coupling between adjacent layers. This stacking arrangement gives rise to quasi-one-dimensional (1D) magnetic chains along the out-of-plane direction, where antiferromagnetic spin waves can be created. Moreover, the electronic structure of CrSBr strongly couples with the internal magnetic order (Fig. 1a). Even subtle spin disturbances originating from the presence of magnons can influence the energy of excitons. This exciton-magnon interaction enables time-resolved optical spectroscopy to serve as a sensitive probe of the magnetic excitations (Fig. 1b). Over the past few years, this experimental method has emerged as a powerful technique to investigate the magnetic structure and dynamics in CrSBr [1]. Traditionally, these studies relied on low-energy excitonic states, which provided limited sensitivity due to the energetic response of only ~ 17 meV.

In our study, we partially lifted this limitation by employing recently uncovered higher-energy excitonic states in CrSBr that exhibit a markedly enhanced sensitivity to magnetization, up to seven times greater than that of their low-energy counterparts (Fig. 1a) [2]. This heightened magneto-optical response dramatically broadens the detectable energy range of magnon-induced perturbations, enabling more efficient tracking of spin-wave dynamics. As a result, these high-energy excitons broaden the avenues for exploring ultrafast spin phenomena and enhance the efficiency in exploring this unusual dynamic of 1D antiferromagnetic spin waves.

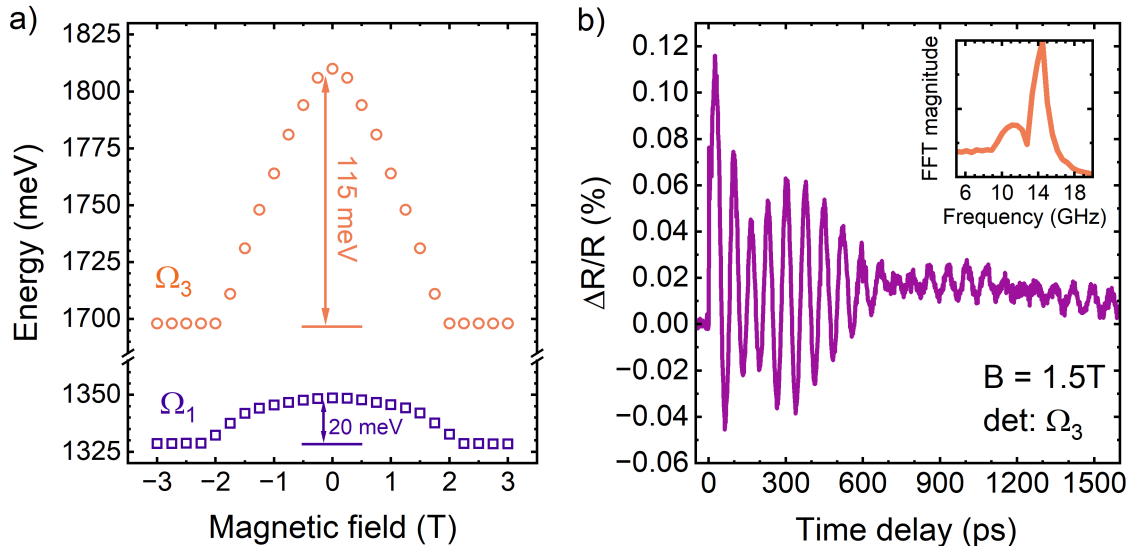


Fig. 1: a) Magnetic field dependence of energy of two excitons in CrSBr: Ω_1 and Ω_3 (notation from [1]). The total energy shift was marked with arrows and written along them. b) Time-dependent lock-in signal from two-color pump-probe experiment on CrSBr. Oscillations in the signal originate from interlayer spin-waves modulating the internal magnetic order, influencing the material's electronic structure. As an in-line figure, the Fourier transform of the signal was included, showing a considerable splitting of the magnon mode (~ 3 GHz), which is visible as the beating in the time-resolved signal.

References [1] Bae, Youn Jue, et al. "Exciton-coupled coherent magnons in a 2D semiconductor." *Nature* 609.7926 (2022): 282-286.
[2] Komar, R., et al. "Colossal magneto-excitonic effects in 2D van der Waals magnetic semiconductor CrSBr." *arXiv preprint arXiv:2409.00187* (2024).

Verification of twisted nematic liquid crystals utility in system to measure the birefringent media

Monika Salamaga^{1,*}, Władysław Artur Woźniak¹

1. Wrocław University of Science and Technology, Wybrzeże Wyspiańskiego 27, 50-370 Wrocław, Poland

Corresponding author: *monika.salamaga@pwr.edu.pl

The one-way double pass Mueller polarimeter is a specific polarimetric setup in that the same module is used as a generator (PSG) and analyzer (PSA) of the different light polarization states. In this setup light passes twice through the test medium and the PSG/PSA due to the reflection from the mirror [1]. At the output of the system, the intensity of light is recorded with a detector (Fig.1).

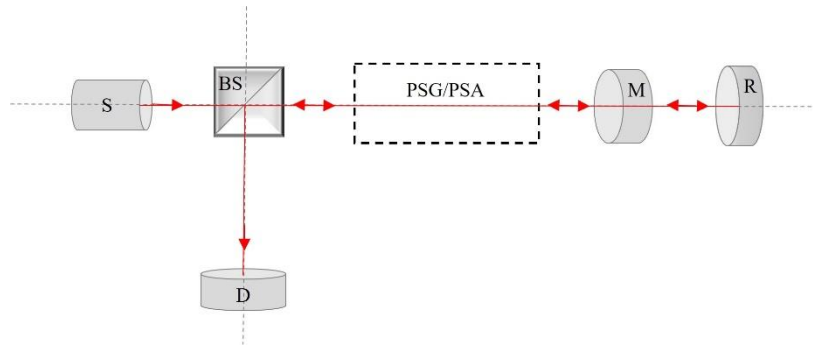


Fig. 1 Generalized schematic of the system: S – source of light, BS – beam splitter, PSG/PSA – polarization state generator and analyzer, M – examined birefringent medium, R – reflective mirror, D – detector.

In the tested system, the PSG/PSA is constructed with a linear polarizer and twisted nematic liquid crystals (TNLCs). Such crystals are an interesting and not popular in Mueller polarimetry alternative to the liquid crystal variable retarders commonly used in polarimetry. The polarization properties of its eigenvectors and the phase difference introduced by them are modified by changing the applied voltage [2]. The practical possibilities of generating and analyzing different light polarization states by the proposed system of polarizer and TNLCs depend on the physical parameters of the liquid crystal cell and change with its 180-degree rotation around the axis. Therefore, based on the measured states possible to be obtained with such a PSG system, a numerical model is created and optimized. Its aim is to determine the best set of PSG/PSA, leading to minimizing the condition number of the system [3]. For the measurements, the obtained from the optimization information about the polarizer's azimuth angle and the set of phases that the TNLC should input is used. Based on the measured light intensities and the Mueller matrix formalism, information about the birefringent properties of the test medium (azimuth and ellipticity angles of its first eigenvector and phase difference introduced between the eigenwaves) is reconstructed. The proposed system was set up, calibrated, and its practical utility was tested by using a medium with well-known properties.

Funding and acknowledgements. This work was supported by the National Science Centre Poland (Reg.no.: 2021/41/N/ST7/03422).

References

- [1] M. Sobczak, P. Kurzynowski, W. A. Woźniak, M. Owczarek, S. Drobczyński, "Polarimeter for measuring the properties of birefringent media in reflective mode", *Opt. Express* **28** (1), 249-257 (2020).
- [2] M. Salamaga, W. A. Woźniak, "Analysis of the possibilities to generate and analyze different polarization states of light by twisted nematic liquid crystal", *Proc. SPIE* 12502 (2022).
- [3] K. M. Twietmeyer, R. A. Chipman, "Optimization of Mueller matrix polarimeters in the presence of error sources", *Opt. Express* **16** (15), 11589 (2008).

Characterization of a Spatially Homogeneous Polariton Condensate in a High-Q GaAs/AlGaAs Microcavity

Piotr Sieradzki^{1,*}, Antonina Bieganowska¹, Hassan Alnatah², Jonathan Beaumariage², David W. Snoke², Michael C. A. Tam³, Zbigniew R. Wasilewski³, Maciej Pieczarka¹

1. Wrocław University of Science and Technology, Wybrzeże Wyspińskiego 27, 50-370 Wrocław, Poland

2. University of Pittsburgh, 3941 O'Hara St., Pittsburgh, PA 15260, USA

3. University of Waterloo, Waterloo, Ontario N2L 3G1, Canada

Corresponding author: *268300@student.pwr.edu.pl

Exciton polaritons are composite quasiparticles originating from coherent light-matter interaction with both light and matter characteristics. They emerge from strong coupling between excitons and photons in semiconductor microcavities. This is the regime at which excitons and photons exchange energy faster than the damping rate of these states. They are bosons, hence enabling polaritons to condense, similar to a Bose-Einstein condensate, in which a macroscopic ground state occupation can be observed, leading to the emergence of spontaneous coherence [1]. We aim to study the interaction-driven phenomena and it is important to generate a high-density and homogeneous polariton condensate, where the interaction energy between condensed polaritons dominates over their kinetic energy. To obtain this, so-called, Thomas-Fermi regime one must utilize a sample with a long polariton lifetime.

In this contribution, by using a high quality GaAs/AlGaAs microcavity [2] and optical trapping technique, we realize a large and homogeneous polariton condensate. We shaped our optical excitation into a ring-shaped spatial profile on the sample, which enabled a repulsive circular potential trapping polaritons. This configuration facilitates the formation of a trapped condensate with a flat top and minimal density changes. Our experimental work includes power-dependent and time-resolved measurements under pulsed excitation conditions, allowing for detailed investigation of condensate formation dynamics and its spatial characteristics.

We manage to observe and characterize the generation of a large, spatially homogeneous polariton condensate exhibiting a low density gradient, whose real space image is demonstrated in Fig. 1. Such systems open new opportunities for exploring hydrodynamical phenomena and spatial fluctuations of the driven-dissipative system [3].

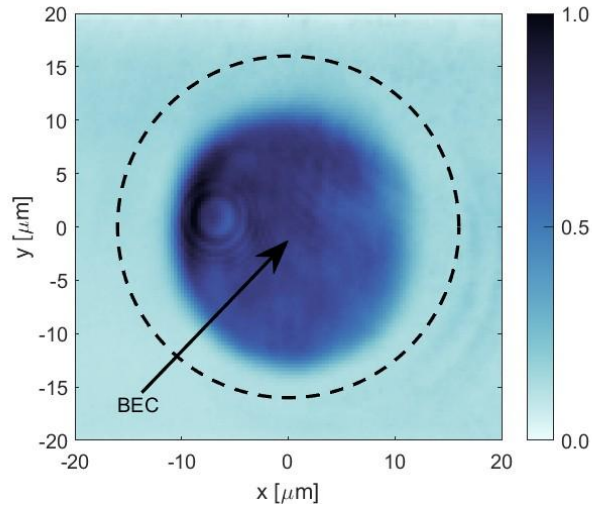


Fig. 1 Real space photoluminescence image of a large and homogeneous exciton-polariton condensate (marked with an arrow) trapped in ring-shaped potential (dashed line) for excitation power above the condensation threshold.

References

- [1] J. Kasprzak et al., “Bose–Einstein condensation of exciton polaritons”. *Nature* 443, 409-414 (2006).
- [2] J. Beaumariage et al., “Measurement of exciton fraction of microcavity exciton-polaritons using transfer-matrix modeling”. arXiv:2406.12940 (2024).
- [3] E. Estrecho et al., “Low-Energy Collective Oscillations and Bogoliubov Sound in an Exciton-Polariton Condensate”. *Phys. Rev. Lett.* 126(7) (2021)

Role of Chlorine Substitution in Tailoring the Optical and Magnetic Properties of CrSBr

Z. Śnioch¹, R. Komar¹, P. Kossacki¹ and T. Kazimierczuk¹

1.Faculty of Physics, University of Warsaw, Warsaw, 02-093 Poland

*Corresponding author: *z.snioch@student.uw.edu.pl*

Two-dimensional materials provide significant versatility in assembling heterostructures, enabling the manipulation of the properties of individual constituent layers. However, they can also benefit from a more classical approach which involves the incorporation of crystals with mixed composition, with the expectation that this will result in a continuous variation of properties across the material.

A prominent 2D material is CrSBr, which has garnered significant research interest in recent years, with numerous studies investigating its unique interplay between semiconducting and magnetic properties[1,2]. It specifically demonstrates highly anisotropic direct-band gap excitations, uniquely coupled with the magnetic sublattice, enabling tunability of the exciton energy via an applied magnetic field. These excitonic interactions occur within the near-infrared spectral range.

In this work, we conduct reflectance measurements on mixed CrSBr crystals, where bromine atoms have been partially substituted with chlorine and iodine. Series of samples with chlorine incorporation levels ranging from 10% to 50%, and one sample with 10% of iodine, allowing us to systematically analyze how this substitution affects the material's optical, and magnetic properties. For all samples, we observed clear exciton features in optical spectra. They were visible in both PL and reflectivity spectra. We determine the parameters of the visible transitions and analyze their variation as a function of composition.

By systematically studying the evolution of excitonic features with increasing halogen substitution, we leverage the strengths of optical techniques to track subtle shifts in energy levels and changes in exciton binding energies, thereby offering a comprehensive characterization of the material's response to compositional tuning.

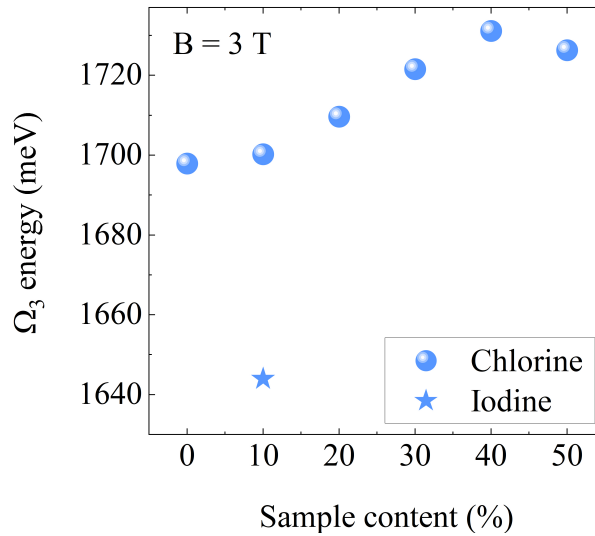


Fig. 1: Example graph illustrating change of exciton energies depending of the chlorine content measured in magnetic field $B = 3$ T

Example References [1] S. Ghimire and D. A. Reis. “High-harmonic generation from solids”. *Nat. Phys.* **15**, 10–16 (2019). For journal articles, authors are listed first, followed by the article’s full title in quotes, the journal’s title abbreviation, the volume number in bold, page number, and the year in parentheses.
[2] G. P. Agrawal, *Nonlinear Fiber Optics*, 3rd. ed., (Academic Press, Boston, 2001). For citation of a book as a whole: authors, followed by title in italics, and publisher, city, and year in parenthesis.
[3] G. P. Agrawal, *Nonlinear Fiber Optics*, chapter 2, 3rd. ed., (Academic Press, Boston, 2001) For citation of a book chapter, authors are listed first, followed by book title in italics, chapter number/name, publisher, city, and year in parenthesis.

Poster session

The effect of cleaning on the transmission properties of blue-control lenses.

inż. Piotr Białucha*, dr inż. Agnieszka Józwiak

Wrocław University of Science and Technology, Wybrzeże Wyspiańskiego 27, 50-370 Wrocław, Poland

Corresponding author: 268203@student.pwr.edu.pl

The modern lifestyle is inherently associated with the extensive use of digital devices, resulting in increased daily exposure to blue light (380-500 nm). This can have a harmful effects on the human visual system. In response to these risks, the development of optical technologies such as blue light filtering lenses has been undertaken. Their effectiveness is dependent, among other factors, on the method of implementing the protective layer and the durability of these coatings under everyday usage conditions.

The objective of this study was to investigate the impact of three commonly used cleaning methods on the light transmission properties of blue light-filtering lenses. Different filtration technologies were analyzed: lens 1 (filter integrated into the lens bulk material, manufacturer 1), lens 2 (filtering layer applied on top of the anti-reflective coating, manufacturer 2), lens 3 (filter embedded within the material structure, manufacturer 2). The study was conducted in the Thin Film Physics Laboratory at Wrocław University of Science and Technology using a UV5100 spectrophotometer over the course of a six-month measurement cycle.

Each lens was subjected to one of the following cleaning methods: water and paper towel (method 1), micro-fiber cloth (method 2) and glass cleaner and paper towel (method 3). The findings indicated that cleaning could result in substantial alterations in light transmission, particularly within the 380-450 nm range. The most substantial effect was observed in lenses with an external filtering layer (lens 2), where transmission increased by up to 10%, which may indicate a reduction in filtration efficiency (Fig. 1). In contact, lenses with a filter integrated into the lens material (lenses 1 and 3) only minor changes were exhibited, suggesting higher resistance to mechanical and chemical degeneration.

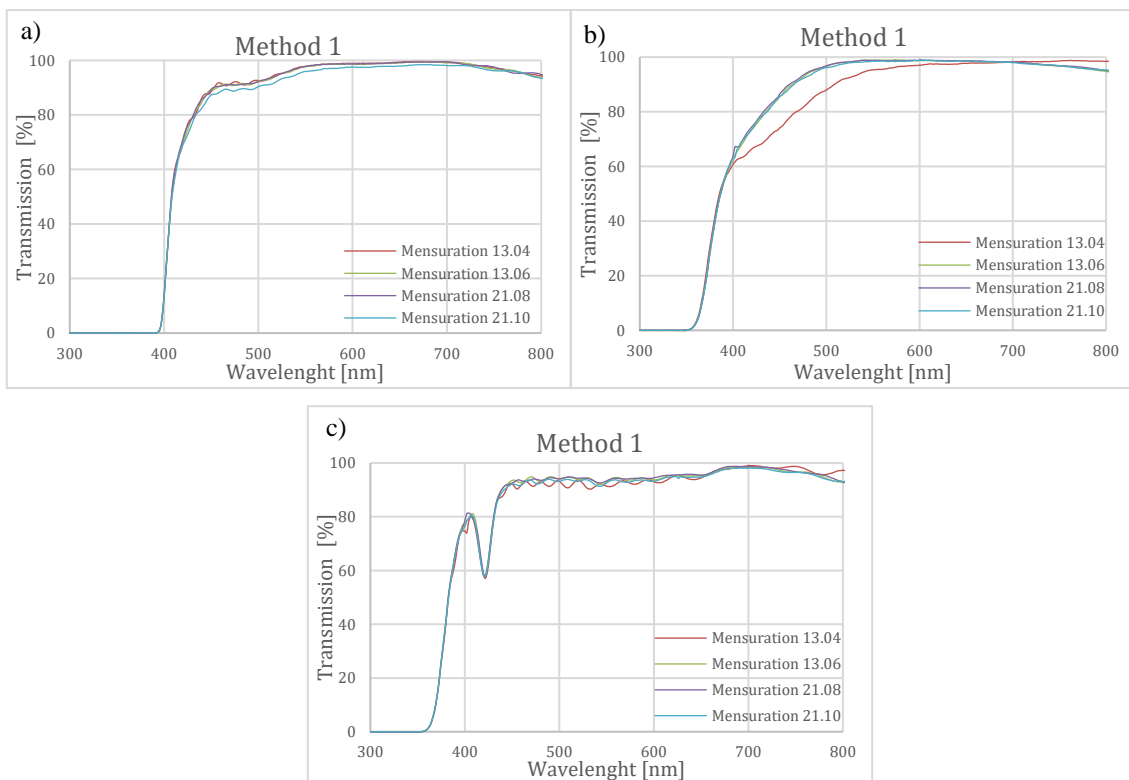


Fig. 1 Results of the six-month measurements for lenses 1-3 method 1, (a) filter integrated into the lens bulk material, manufacturer 1, (b) filtering layer applied on top of the anti-reflective coating, manufacturer 2, (c) filter embedded within the material structure, manufacturer 2

The findings underscore the necessity of incorporating lens manufacturing technology into the formulation of care recommendations. The adaptation of cleaning methods to the specific characteristics of protective coatings has been demonstrated to significantly influence the preservation of their filtering properties and ensure long-term user comfort.

Not only plasmonics: how metal nanoparticles influence the performance of ferro-pyro-phototronic detectors

Adrian Kaim^{1*}, Katarzyna Gwóźdz¹, José B.P. Silva^{2,3}

1. Department of Experimental Physics, Wrocław University of Science and Technology, Wyb. Wyspińskiego 27, 50-370 Wrocław, Poland

2. Physics Center of Minho and Porto Universities (CF-UM-UP), University of Minho, Campus de Gualtar, Braga, 4710-057 Portugal

3. Laboratory of Physics for Materials and Emergent Technologies, LapMET, University of Minho, Braga, 4710-057 Portugal

Corresponding author: *adrian.kaim@pwr.edu.pl

Photodetectors are fundamental components in a wide range of optical systems, enabling applications from imaging and communication to sensing and optical signal processing. Conventional detectors, such as simple photodiodes, typically require an external bias voltage for efficient operation. To reduce electrical energy consumption, researchers are increasingly exploring self-powered alternatives. One promising approach is to use additional electric field sources — such as pyroelectric and ferroelectric effect — to enhance the built-in electric field within the semiconductor junction, which the photovoltaic effect is based on. This enhancement improves the separation of photo-generated charge carriers, thus boosting overall efficiency of so-called ferro-pyro-phototronic detectors. The ferro-pyro-phototronic effect can be observed in structures combining materials such as pyroelectric ZnO and ferroelectric BCZT ($0.5\text{Ba}(\text{Zr}_{0.2}\text{Ti}_{0.8})\text{O}_3-0.5(\text{Ba}_{0.7}\text{Ca}_{0.3})\text{TiO}_3$), where the performance of the device is strongly influenced by the polarization state of the ferroelectric component [1]. Another strategy for enhancing photodetection efficiency involves metallic nanoparticles. These particles exhibit plasmonic effect, which can improve light absorption at wavelengths related to the plasmon resonance frequency, while also acting as an additional electric field source [2]. However, introduction of the plasmonic nanoparticles into the device also alters other phenomena occurring within the structure, potentially enhancing or degrading photodetector performance. Notably, changes in nanoparticle placement, as presented in figure 1a, may lead to the disappearance of the ferroelectric properties of the device. This study investigates the photocurrent generated by the detector structures with and without silver nanoparticles under modulated laser illumination (figure 1b). Response to changes in ferroelectric polarization is analyzed. A mechanism responsible for the diminishing of the ferroelectric component will be presented.

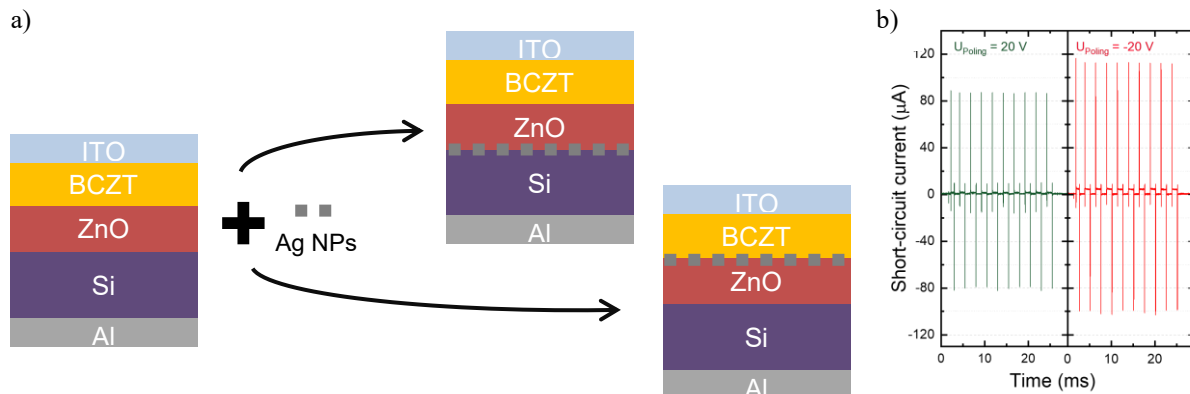


Fig. 1 (a) Detector structures studied in this work. (b) An example of a short-circuit current signal obtained under pulsed 650 nm laser illumination from the ITO/BCZT/ZnO/Si/Al detector at two opposing ferroelectric polarization states.

Funding and acknowledgements.

The work was supported by the project Minigrants for doctoral students of the Wrocław University of Science and Technology.

References

- [1] A. Kaim, K. Gwóźdz, E. M. F. Vieira, and J. P. B. Silva, “Ferroelectric effect in oxide based pyro-phototronic photodetector,” *Przegląd Elektrotechniczny*, vol. 1, no. 10, pp. 251–253, Oct. 2023, doi: 10.15199/48.2023.10.51.
- [2] J. P. B. Silva *et al.*, “High-performance and self-powered visible light photodetector using multiple coupled synergetic effects,” *Mater Horiz*, vol. 11, no. 3, pp. 803–812, 2024, doi: 10.1039/D3MH01725G.

Simple and Effective Tissue Attenuation Measurement

Uliana Finaeva¹, Sarka Nemcova¹, Jiri Cap¹, Petr Denk¹, Jan Dvorak¹

¹ Czech Technical University in Prague, Technicka 4, 16000 Prague, Czech Republic

Corresponding author: *uliana.finaeva@fs.cvut.cz

Our study focuses on measuring optical transmittance using a compact 3D printed device and evaluating the attenuation coefficient from acquired data. This low-cost method offers an alternative to more traditional equipment (e.g., Integrating sphere, fiber to fiber measurements), with results agreeing with existing literature. Measurement and calculation approaches are validated on several different white rat cadaver tissues. Spectral transmissivity measurement of metastasis model in liver is performed showing the possibility of differentiation between healthy and diseased matter with given simple method. The measurements of white rat spleen light attenuation are performed in VIS and NIR spectra that were not yet reported in literature.

Although the Beer-Lambert law (Eq.1) deals mainly with absorption, it can be used to model the attenuation of light in tissues, which results from both absorption and scattering effects [26-28]; therefore, μ [mm^{-1}] (Eq.2) is presented as an attenuation coefficient. Thanks to the simplicity and linearity, the Beer-Lambert law allows for the straightforward assessment of how different wavelengths of light interact with tissue, allowing for spectral characterization. We measured transmissivity (Eq. 3) and roughly measured the thickness of sample b deriving the attenuation coefficient of tissue.

$$I = I_0 e^{-\mu b} \quad (1)$$

$$\mu = \mu_s + \mu_a \quad (2)$$

$$T = \frac{I}{I_0} * 100\% \quad (3)$$

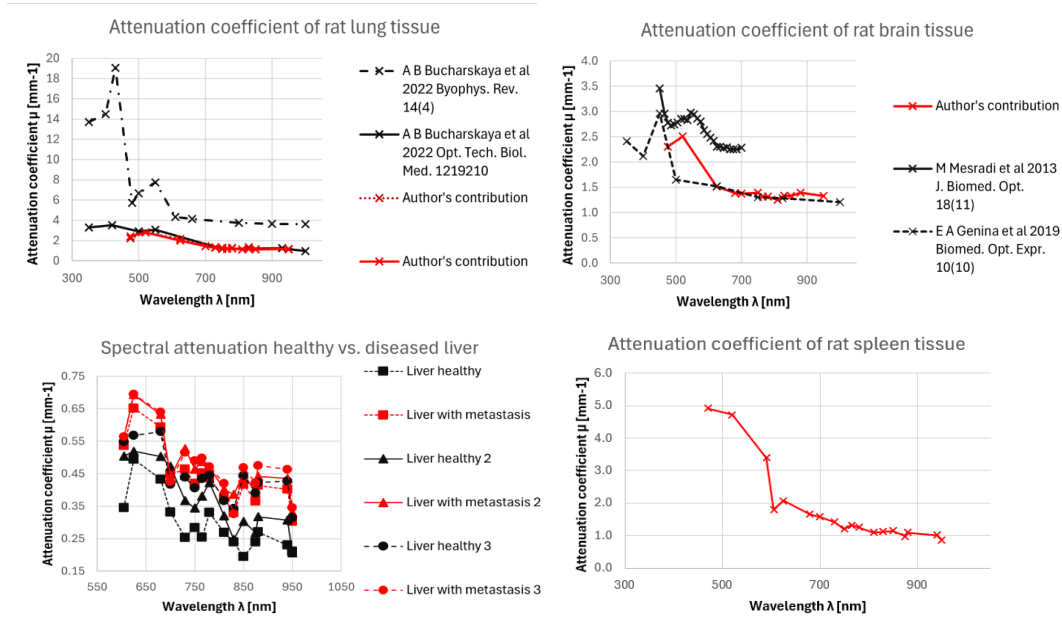


Fig. 1 Spectral attenuation coefficient of white rat tissues: Validation of the chosen method by comparison to reported data: (a), (b); Healthy and metastatic tissue differentiation (c); The newly reported white rat spleen spectral attenuation in VIS and NIR: (d).

Statement on Ethical Treatment of Animals: The materials of white rats were obtained from cadavers, remaining from other experiments, where the killing method did not influence internal organ optics.

References

- [1] E. A. Genina et al. "Optical properties of brain tissues at the different stages of glioma development in rats: pilot study". In: Biomed Opt Express 10 (2019), pp. 1–10. doi: 10.1364/BOE.10.005182.
- [2] L. Ntombela, B. Adeleye, and N. Chetty. "Low-cost fabrication of optical tissue phantoms for use in biomedical imaging". In: Heliyon 6 (2020), e03602. doi: 10.1016/j.heliyon.2020.e03602.
- [3] A. M. K. Nilsson, R. Berg, and S. Andersson-Engels. "Measurements of the optical properties of tissue in conjunction with photodynamic therapy". In: Appl Opt 34 (1995), pp. 4609–4619. doi: 10.1364/AO.34.004609.

Hydrostatic pressure and temperature cross-sensitivity in Rayleigh scattering-based distributed fiber measurements

Agnieszka Bednarek¹, Małgorzata Garbaca^{1,2}, Marta Bernaś¹, Paweł Mergo³,
Jacek Olszewski¹, Gabriela Statkiewicz-Barabach¹

1. Wrocław University of Science and Technology, Wybrzeże Stanisława Wyspiańskiego 27, 50-370 Wrocław, Polska

2. SHM System, ul. Jana Pawła II 82A, 30-444 Libertów

3. Laboratory of Optical Fiber Technology, Maria Curie-Skłodowska University, pl. M. Curie-Skłodowskiej 3, 20-031 Lublin, Poland

Corresponding author: agnieszka.bednarek@pwr.edu.pl

The applicability of a birefringent **K-type side-hole fiber (SHF)** for hydrostatic pressure and temperature distributed sensing based on Rayleigh scattering is investigated. The aim is to determine the fiber's sensitivities to aforementioned parameters and ensure the difference in the fiber's response is sufficient to differentiate which parameter caused the change.

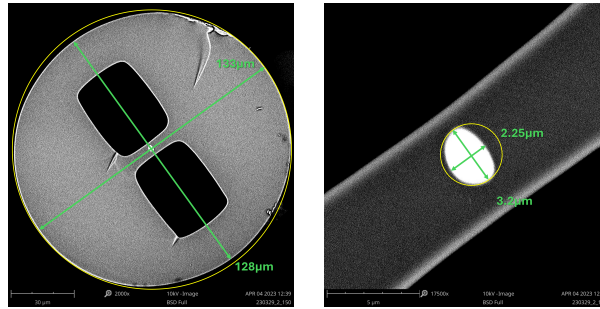


Fig. 1: Dimensionalized SEM pictures of the fiber.

The K-type SHF developed and studied by us is characterized by a record difference in response to hydrostatic pressure for two orthogonal polarization modes due to the placement of two large air holes in a sufficiently close distance from the core. Moreover, due to the appropriate orientation of the core relative to the holes (K-type), the sign of the differential sensitivity is positive, which results in an increase in birefringence with increasing pressure. Thanks to this, there is no danger that the birefringence induced by the pressure increase will compensate for the birefringence of the fiber itself, which could significantly limit the pressure measurement range.

The tested fiber, measured at atmospheric pressure, shows closely same nonlinear response to temperature, in the range of 20-250°C, for both orthogonal polarization modes, amounting to about -1.5 GHz/°C. The fiber's responses to changes in hydrostatic pressure in the range of 0.1-20 MPa, measured at room temperature, for orthogonal polarization modes are linear, have opposite signs and amount to about -1.9 GHz/MPa and 0.8 GHz/MPa.

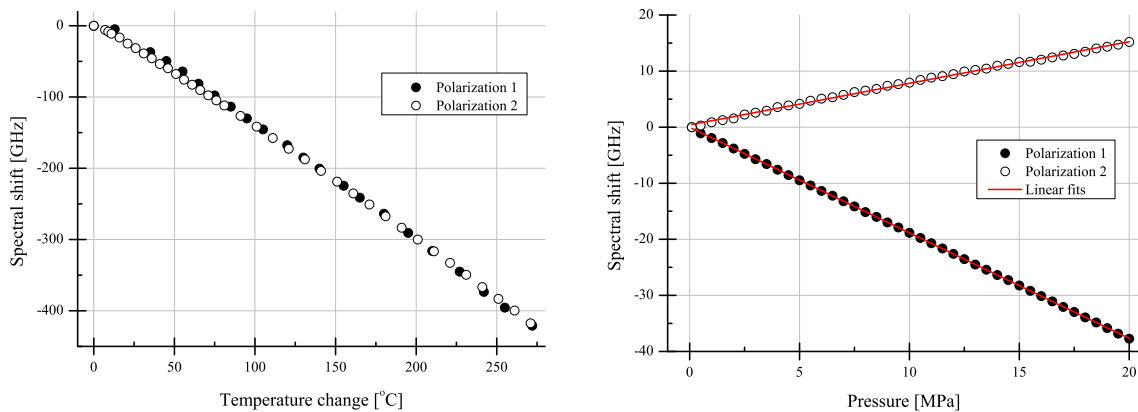


Fig. 2: Obtained relations between the fiber's response and applied changes of temperature and hydrostatic pressure.

Research funds provided by:

Fundation for Polish Science (FENG.02.07-IP.05-0139/23) and

National Science Centre (Grant Opus 18, DEC-2019/35/B/ST7/04135)

Design of fiber-based dispersive elements for quantum information science

Antoni Skoczypiec¹, Michał Karpiński^{1,*}

1. Faculty of Physics, University of Warsaw, Pasteura 5, 02-093 Warszawa, Poland

Corresponding author: *michal.karpinski@fuw.edu.pl

Fiber Bragg gratings (FBGs) are fiber-based dispersive elements that have a range of applications in telecommunication and sensor construction. Modifications to uniform FBGs result in different phase and spectral responses, allowing for the construction of dispersion-compensating filters, pulse shapers and multiplexers. At the same time, high sensitivity to external conditions – temperature and stress – makes them perfect to use as temperature, strain, acceleration or magnetic field sensors [1]. In each of these applications, certain grating properties are desirable, such as low dispersion, high reflectance at the maximum, absence of sidebands, or particular dispersion profile for pulse shaping [2]. This is not always easy to achieve, so it is crucial to understand characteristics and develop methods to design FBGs with the desired parameters.

In this work I present a genetic algorithm which can design a Bragg grating, given its parameters, such as length, spectrum and wavelength-dependent phase response. In particular, the algorithm can improve desired parameters starting from already known grating designs. The genetic algorithm involves incremental enhancement of some initial population of FBG designs by crossover and mutation. The optimization is run with objective function

$$d(\text{calc}, \text{target}) = a d_{p_1}(R_{\text{calc}}, R_{\text{target}}) + (1 - a) d_{p_2}(\varphi_{\text{calc}}, \varphi_{\text{target}}), \quad (1)$$

where $R_{\text{calc}}, R_{\text{target}}$ are our design's and target spectra, $\varphi_{\text{calc}}, \varphi_{\text{target}}$ respective phase responses and $d_p(\cdot, \cdot)$ is the p -norm. Such formulation allows for tuning weights for spectrum error, phase error, etc., and adding more penalty terms, e.g. for maximal dispersion.

On the poster I show several examples of algorithmically synthesized designs, which turn out to have better performance than filters with known apodization profiles. One of them is bandpass filter with low dispersion, which is shown on Fig. 1. The resulting design has maximal dispersion of $420 \frac{\text{ps}}{\text{nm}}$ which is about 10 times lower than for a sine-apodized grating of the same length.

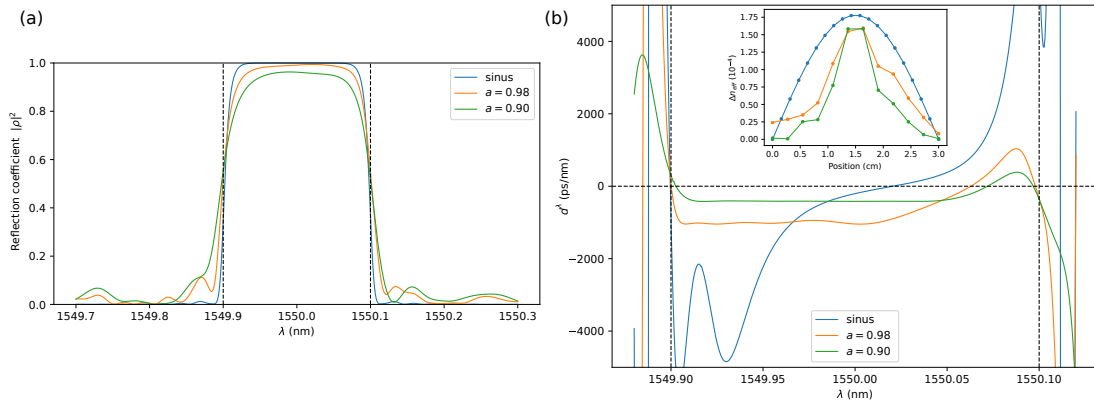


Fig. 1: (a) Spectrum and (b) dispersion of bandpass filters optimized for low dispersion, compared with sine-apodized grating. The parameter a is the weight of spectrum error in the objective function, i. e. lower a puts more importance on low dispersion during optimization.

To verify the validity of the algorithm, I also measured spectrum and index modulation of a chirped FBG fabricated at University of Southampton [3] and compared it with synthetic results. This shows that the developed algorithm can be used to design Bragg gratings with desirable parameters for sensing and as a part of larger photonic systems, such as a high-resolution single-photon spectrometer [4] or an interface between quantum light pulses with different timescales or spectral-temporal profiles [2, 5].

References

- [1] R. Kashyap, *Fiber Bragg Gratings*, 2nd. ed., (Academic Press, 2010).
- [2] M. Karpiński et al., “Control and Measurement of Quantum Light Pulses for Quantum Information Science and Technology”, *Adv. Quantum Technol.* **4**, 2000150 (2021).
- [3] C. Sima et al., “Ultra-wide detuning planar Bragg grating fabrication technique based on direct UV grating writing with electro-optic phase modulation”, *Opt. Express* **21**, 15747–15754 (2013).
- [4] A. O. C. Davis et al., “Pulsed single-photon spectrometer by frequency-to-time mapping using chirped fiber Bragg gratings”, *Opt. Express* **25**, 12804–12811 (2017).
- [5] F. Sośnicki et al., “Interface between picosecond and nanosecond quantum light pulses”, *Nat. Photon.* **17**, 761–766 (2023).

Development of a Mirror Inside Anti-Resonant Hollow Core Fiber

Piotr Perehiniec^{1,*}, Patrycja Gronowicz¹, Ryszard Buczyński², Michał Nikodem¹

1. Wrocław University of Science and Technology, Wybrzeże Wyspiańskiego 27, 50-370 Wrocław, Poland

2. Institute of Microelectronics and Photonics, Warsaw and University of Warsaw

Corresponding author: *piotr.perehiniec@pwr.edu.pl

In recent years, ARHCFs (Anti-Resonant Hollow Core Fibers) have attracted significant interest, primarily due to their potential applications in optical telecommunication. Another emerging area of interest is their use in sensing, particularly gas sensing via laser absorption spectroscopy. In such systems, light passes through a region containing molecules of unknown concentration. As the light reaches the detector, an absorption spectrum is recorded, from which the molecular concentration can be determined using Beer–Lambert’s law. The basic setup typically includes a light source, a gas cell, and a detector. Traditionally, the gas cell is a bulky glass chamber, often equipped with internal mirrors to form a multi-pass cell that increases the effective sensing path length. Recently, ARHCFs have been proposed as a compact alternative to conventional gas cells [1].

In certain configurations, it may be advantageous to use ARHCFs in a reflective setup [2], where a mirror is placed at one end of the fiber so that light enters and exits from the same side. In this work, we propose using a tapered solid-core fiber (SCF) as the reflective element. The concept is illustrated schematically in Fig. 1. First, a standard SCF is tapered, cleaved, and coated with a gold layer, to work as a mirror. The coated fiber is then inserted into the hollow core of the ARHCF. Finally, the connection is permanently fused by localized heating. Additionally, a side-hole can be fabricated in the ARHCF to allow gas to enter the fiber core for sensing purposes.

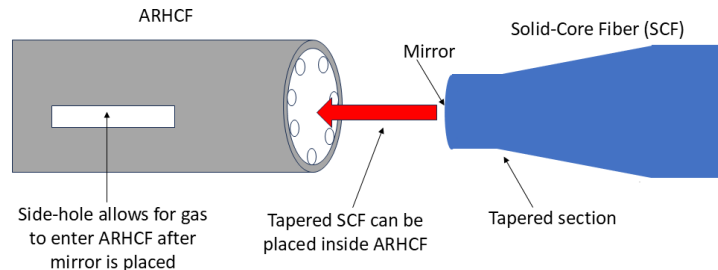


Fig. 1 Schematic diagram showing ARHCF with a mirror made from tapered solid-core fiber.

In our work, we utilize the Fujikura LZM-100 CO₂ splicer to fabricate the taper and connect it with the ARHCF. In our current experiments, we have successfully tapered a standard solid-core fiber (SCF) and inserted it into the ARHCF, though the gold coating has not yet been applied. Figure 2 presents the cross-section of the ARHCF (with an outer diameter of 125 μm), a side view of the fiber, and an image showing the tapered SCF positioned inside the ARHCF. The reflection from the SCF’s end facet was verified using a LUNA OBR 4600 Optical Backscatter Reflectometer.

These are proof-of-concept experiments, that we now plan to repeat using a gold-coated tapered SCF to enhance mirror reflectivity. Additionally, a side-holes in the ARHCF will be made using a focused ion beam (FIB), to enable gas flow through the fiber core for gas sensing experiments.

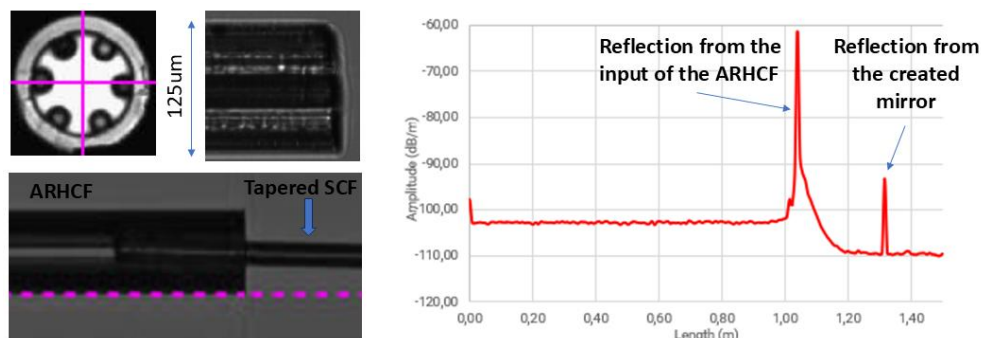


Fig. 2 Left: pictures of the ARHCF and the picture of the tapered solid-core fiber inserted inside ARHCF. Right: graph of a LUNA’s back scattering signal with two reflections visible: the one from the input of the ARHCF (this is reflection from a fiber that was used to connect LUNA with ARHCF), and the other reflection from the mirror created with a tapered SCF.

References

- [1] P. Jaworski. “Review of Antiresonant Hollow-Core Fiber-Assisted Spectroscopy of Gases”. *Sensors* 21, 5640 (2011).
- [2] G. Gomółka, D. Pysz, R. Buczyński, and M. Nikodem, “Dual-Pass Hollow-Core Fiber Gas Spectroscopy Using a Reflective Configuration With Heterodyne-Based Signal Detection,” *J. Lightwave Technol.* 41, 6094-6101 (2023)

Optical vortex trajectories as indicators of wavefront aberrations

Aleksandra K. Korzeniewska¹, Magdalena Łukowicz¹, Kamil Kalinowski¹, Karolina Gemza¹, Mateusz Szatkowski¹

1. Wrocław University of Science and Technology, Wybrzeże Wyspiańskiego 27, 50-370 Wrocław, Poland

Corresponding author: *aleksandra.korzeniewska@pwr.edu.pl

An optical vortex is a point in an optical field where the phase of the wave is undefined and the beam intensity drops to zero. The position of this singularity during beam propagation is highly sensitive to external perturbations, which leads to a displacement of the vortex core [1]. The vortex trajectory is defined as the displacement of the phase discontinuity point in the detector plane as the vortex-generating element is displaced perpendicular to the optical axis [2]. As demonstrated in [3], vortex trajectories provide an objective method for assessing beam quality. Any optical system equipped with a spatial light modulator or a micromirror array can utilize the proposed method to evaluate the beam quality.

In our work, we conducted a numerical analysis of the influence of individual aberrations—astigmatism (Z_2^2), defocus (Z_2^0), and coma (Z_3^1)—on vortex trajectories. The experimental setup is shown in Fig.1a). A beam with aberrations introduced by element A propagates through a spiral phase plate (SPP), which is laterally displaced off the optical axis in two orthogonal directions, perpendicular to the beam propagation. The position of the phase singularity was observed on a stationary CCD detector. Fig.1b) illustrates shows the impact of the considered aberrations on the recorded trajectories. In this work, we quantitatively linked unique features of the trajectories to specific aberrations.

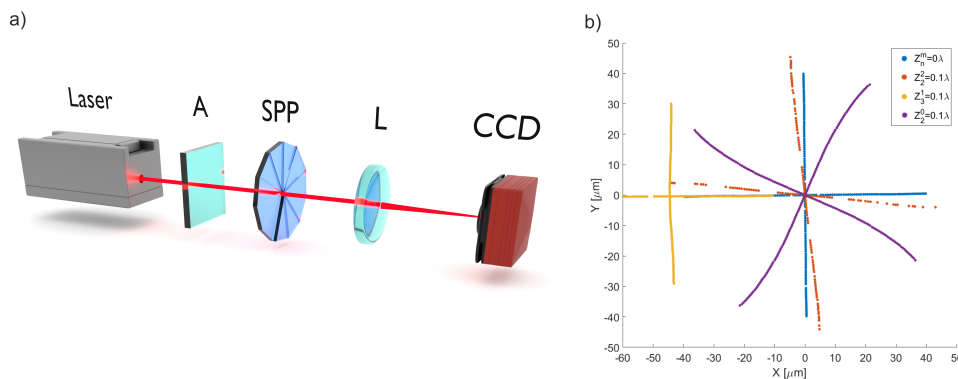


Fig. 1: (a) Schematic of the setup for measuring optical vortex trajectories: A—refractive element introducing aberration, SPP—spiral phase plate generating the vortex, L—lens, CCD—detector. (b) Optical vortex trajectories for different aberrations, recorded while translating the phase plate in two orthogonal directions perpendicular to the beam propagation axis.

Using the specific response of vortex trajectories to defocus, we propose an autofocusing algorithm, which utilizes the phase singularity behaviour, an objective parameter linking particular quantity with the focal plane. The beam propagated through a spiral phase plate (SPP) with a fixed lateral displacement. The trajectory of the dark core (i.e., the position of the phase discontinuity along the optical axis) was recorded by translating the detector in the vicinity of the system's focal plane. The numerical results were validated experimentally.

Funding and acknowledgements. This research was funded in whole by National Centre for Research and Development, 0230/L-13/2022.

References:

- [1] A. Popiołek-Masajada, J. Masajada, and M. Szatkowski. "Internal scanning method as unique imaging method of optical vortex scanning microscope." *Optics and Lasers in Engineering* 105 (2018): 201-208.
- [2] Ł. Płociniczak, et al. "Analytical model of the optical vortex microscope." *Applied optics* 55.12 (2016): B20-B27.
- [3] M. Szatkowski, A. Popiołek-Masajada, and J. Masajada. "Optical vortex trajectory as a merit function for spatial light modulator correction." *Optics and Lasers in Engineering* 118 (2019): 1-6.

Wavefront sensing with optical vortices leads to improved shot noise resistance

Magdalena Łukowicz^{1,*}, Aleksandra Korzeniewska¹, Kamil Kalinowski¹, Rosario Porrás-Aguilar², Mateusz Szatkowski¹

1. Wrocław University of Science and Technology, Wybrzeże Wyspińskiego 27, 50-370 Wrocław, Poland

2. The University of North Carolina at Charlotte, Department of Physics and Optical Science, Charlotte, North Carolina, 28223, USA

Corresponding author: *magdalena.lukowicz@pwr.edu.pl

In optical metrology, we use two types of devices which can be used to measure the wavefront of the beam. The first one is based on interferometric methods [1], while the other one analyzes the incident angle. The representative of the second group is the Shack-Hartmann wavefront sensor [2], which uses the matrix of microlenses to reconstruct the shape of the wavefront. It analyzes the displacement of every single point focused by the matrix of microlenses in relation to its reference position. A key part of this method is to precisely pinpoint the focused spots, because even small inaccuracies can lead to phase errors.

In this work we propose a different geometry of the probing beam. We use Laguerre-Gaussian beam [3] in our new sensor based on Shack-Hartmann sensor architecture. The Laguerre-Gauss includes phase discontinuities, which exhibit a high sensitivity to phase disturbances, moreover they provide new localization possibilities.

Our proposed localization method relies on determining the position of the point by taking into account information about the presence of the phase singularities and constructing pseudo-complex amplitude [4].

In this study we compare the effectiveness of detecting the position for classic gaussian beam which was localized by the center of gravity method [5] and Laguerre-Gauss beam, through the proposed method. The examples of both beam matrices and their detected centers are presented in Fig. 1. We perform both, numerical simulations and experimental tests.

Based on that, we further examine the effectiveness of the vortex-based Shack-Hartmann sensor in the presence of controlled shot noise.

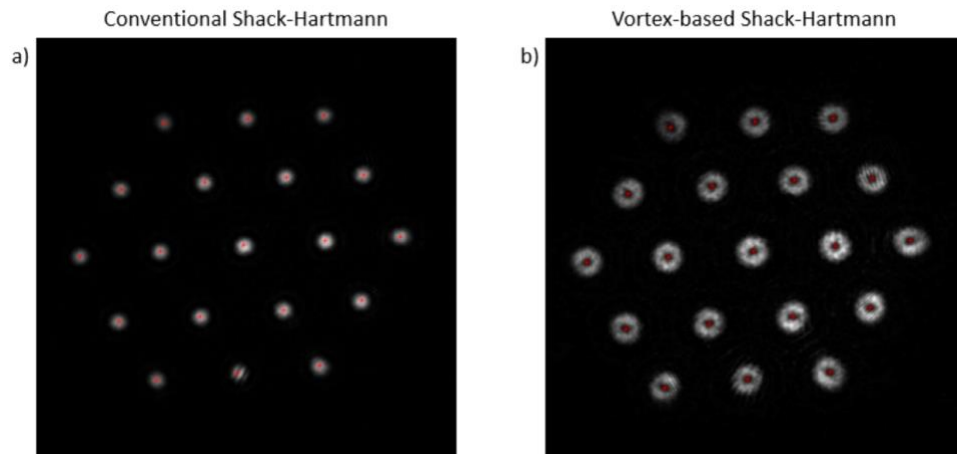


Fig. 1 (a) Conventional Shack-Hartmann with marked centers found using the center of gravity method. (b) Vortex-based Shack-Hartmann with marked singularity positions, detected using our proposed localization approach.

Funding and acknowledgements. This research was funded by the National Centre for Research and Development, grant no. 0230/L-13/2022.

References

- [1] K. L. Baker, "Interferometric wavefront sensors for high contrast imaging," *Opt. Express* 14, 10970-10975 (2006).
- [2] A. Aghajani, F. D. Kashani, and M. Yousefi, "Laboratory study of aberration calculation in underwater turbulence using Shack-Hartmann wavefront sensor and Zernike polynomials," *Opt. Express* 32, 15978-15992 (2024).
- [3] G. J. Gbur, *Singular Optics* (1st ed.). CRC Press (2016).

Photoresponse properties of various azo-dyes dispersed in different polymer matrices

Seyede Jahani^{1,*}, Dariusz Chomicki¹, Jolanta Kowalonek², Robert Czaplicki¹, Vitaliy Smokal³, Beata Derkowska-Zielinska^{1,#}

1. Institute of Physics, Faculty of Physics, Astronomy and Informatics, Nicolaus Copernicus University in Torun, Grudziadzka 5/7, 87-100 Torun, Poland

2. Faculty of Chemistry, Nicolaus Copernicus University in Torun, Gagarina 7, 87-100 Torun, Poland

3. Faculty of Chemistry, Taras Shevchenko National University of Kyiv, 64/13 Volodymyrska St., 01601 Kyiv, Ukraine

Corresponding author: *arastehjahani79@gmail.com; #beata@fizyka.umk.pl

Azobenzene is an aromatic molecule that consists of two phenyl rings linked by an azo bridge that allows for the existence of its two isomeric forms: stable *trans* and metastable *cis*. This compound represents well a broad family of molecules that are characterized by the ability to undergo reversible photoisomerization between *trans* and *cis* configurations upon exposure to specific wavelengths of light. Such ability causes significant changes in their physical and chemical properties and underlies their widespread use in photonic devices, optical storage, and molecular switches [1, 2].

We study the photophysical properties of azo dyes such as Disperse Red 1, Disperse Red 13, and Disperse Orange 3 dispersed in polymer matrices of chitosan, poly(methyl methacrylate) (PMMA), and poly(4-vinylpyridine) (P4VP). Such polymers were selected due to their compatibility with azobenzene derivatives and the ability to form uniform thin films. The obtained host-guest systems combine the photoresponsive behavior of azobenzene dyes with the mechanical and functional versatility of the polymer hosts, enabling the study of light-induced phenomena in thin films (see Fig. 1) [3].

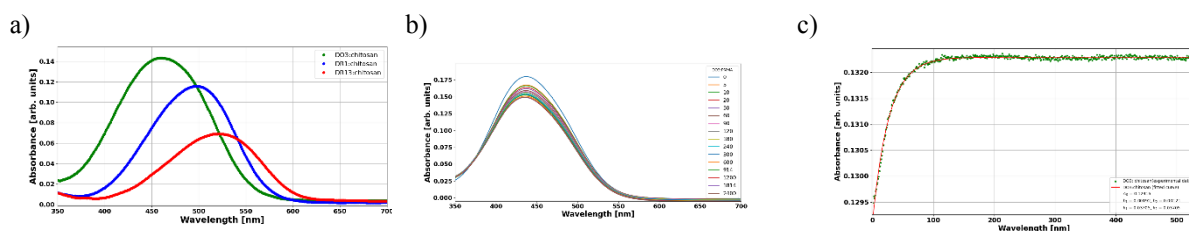


Fig. 1 (a) Absorption spectra of azo dyes dispersed in chitosan matrix. (b) Absorption spectra of DO3 dispersed in PMMA matrix during sample irradiation. (c) Absorbance growths during relaxation in the darkness at the maximum absorption wavelength before irradiation for DO3:chitosan.

The spin-coated thin films of azo dyes exhibit uniform dispersion of azo dyes within the polymer matrices, which was verified by atomic force microscopy study. As expected, when films were exposed to laser light of a wavelength absorbed by azo dye, the molecules displayed strong photoisomerization, enabling the formation of surface relief gratings. Atomic force microscopy images confirmed the light-induced surface patterns. These results demonstrate that combining azo dyes with polymers such as chitosan, PMMA, and P4VP allows obtaining advanced materials with tunable optical properties and surface morphologies, which opens promising opportunities for innovative applications in biomedicine, photonics, and beyond [4-6].

References

- [1] D. Chomicki, O. Kharchenko, L. Skowronski, J. Kowalonek, A. Kozanecka-Szmigiel, D. Szmigiel, V. Smokal, O. Krupka, B. Derkowska-Zielinska. "Physico-Chemical and Light-Induced Properties of Quinoline Azo-dyes Polymers". *Int. J. Mol. Sci.* 21, 5755 (2020).
- [2] D. Chomicki, O. Kharchenko, A. Kaczmarek-Kędziera, R. Czaplicki, O. Krupka, D. Kowalska, S.A. Jahani, V. Smokal, B. Derkowska-Zielinska. "Thermal isomerization rates of new azoquinoline functionalized copolymers as a function of substitution patterns". *ChemPhysChem* 2025 DOI: 10.1002/cphc.202401155
- [3] M. Kim, C. Hillel, K. Edwards, W. Pietro, O. Mermut, C.J. Barrett. "Chitosan-azo dye bioplastics that are reversibly resoluble and recoverable under visible light irradiation". *RSC Adv.* 14, 25771-25784 (2024).
- [4] N.R.A. Atmah, W.R. Caliman, A. Pawlicka, R.G. Sabat, J.-M. Nunzi. "Surface relief grating on chitosan-N,N-dimethyl-4-(2-pyridylazo)aniline thin film". *Polymers* 14, 791 (2022).
- [5] B. Derkowska-Zielinska, A. Kozanecka-Szmigiel, D. Chomicki, V. Smokal, Y. Kawabe, O. Krupka. "Effect of 2-Methylthiazole Group on Photoinduced Birefringence of Thiazole-Azo Dye Host-Guest Systems at Different Wavelengths of Irradiation". *Molecules* 27, 6655 (2022).
- [6] B. Derkowska-Zielinska, O. Krupka, V. Smokal, A. Grabowski, M. Naparty, L. Skowronski. "Optical properties of disperse dyes doped poly(methyl methacrylate)". *Mol. Cryst. Liq. Cryst.* 639, 87-93 (2016).

INVESTIGATION OF LIGHT ILLUMINATION EFFECTS ON ELECTRICAL PROPERTIES OF WSe₂ AND MoS₂ – ANALYSIS OF CURRENT-VOLTAGE CHARACTERISTICS

Karolina Nietubyć, Kinga Majkowycz

u57303@student.wat.edu.pl

Two-dimensional materials from the transition metal dichalcogenide (TMDC) group, such as tungsten diselenide (WSe₂) and molybdenum disulfide (MoS₂), exhibit promising properties for photodetection applications. These materials can be utilized in fields like electronics, space industry, environmental monitoring, medicine, and security systems, offering innovative approaches to infrared radiation detection.

In this study, WSe₂ and MoS₂ flakes were exfoliated onto Si/SiO₂ substrates. Pt/Au electrical contacts were fabricated on the 2D material flakes using electron beam lithography (Fig. 1b). The current-voltage (I-V) characteristics of the materials were measured under various illumination conditions: daylight and lasers with different wavelengths—blue (~470 nm), green (~530 nm), and red (~625 nm).

The results indicate that both WSe₂ and MoS₂ exhibit varied responses depending on the light wavelength, which is related to their band structure and bandgap energy.

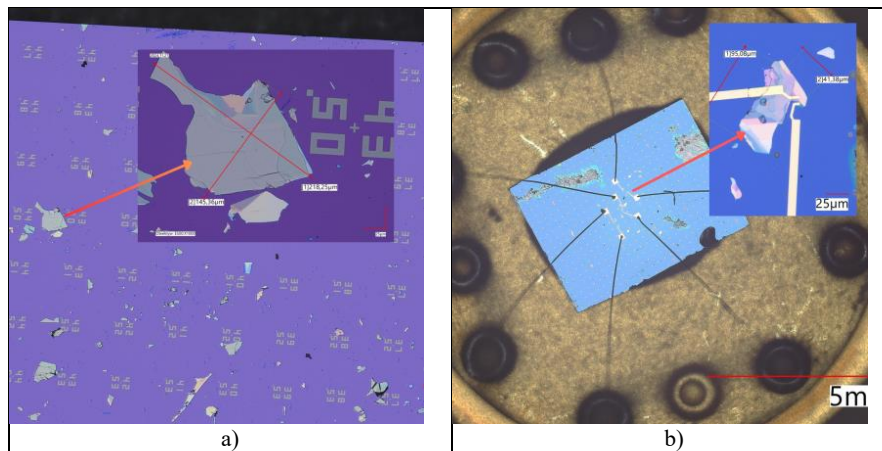


Fig. 1: (a) Optical microscope image of WSe₂ flake on Si/SiO₂ substrate at 80x and 1000x magnification. (b) WSe₂ flake with fabricated Pt/Au contacts for I-V measurements.

3D-print nanoWaste: Multiscale Investigation of Nano-/Microplastic Formation, Composition, and Toxicity in Polymer-Based Additive Manufacturing

Piotr Kalużyński¹, Daria Kalużyńska^{2,3,5}, Przemysław Nowakowski^{1,4}, Wiktoria Szyska¹, Anna Wiszkony⁵

1. Department of Optoelectronics, Silesian University of Technology, 44-100 Gliwice, Poland

2. Biotechnology Center, Silesian University of Technology, 44-100 Gliwice, Poland,

3. Maria Skłodowska-Curie National Research Institute of Oncology, 44-102 Gliwice,

4. IPG Photonics Sp. z o.o., Leona Wyczółkowskiego 8, 44-109 Gliwice, Poland

5. Faculty of Automatic Control, Electronics and Computer Science, Silesian University of Technology, 44-100 Gliwice, Poland

Corresponding author: pkaluzynski@polsl.pl

The accelerating adoption of 3D printing technologies, particularly Fused Deposition Modeling (FDM) and Digital Light Processing (DLP), has unlocked transformative capabilities in rapid prototyping, biomedical engineering, and consumer product manufacturing. Despite these advances, emerging evidence indicates that 3D printing may also serve as a previously underestimated source of nano- and microplastic (NMP) pollution. These contaminants – defined as plastic particles smaller than 5 mm – are not only by-products of long-term environmental degradation but can also form directly during the additive manufacturing process.

In resin-based systems such as DLP, routine post-processing workflows – including solvent washing and UV curing – may catalyze the formation of NMPs from residual, partially polymerized resin. Our investigations reveal that contact between liquid resin and alcohols like isopropanol or ethanol, followed by photo-crosslinking, induces spontaneous polymer precipitation. The resulting dispersions contain both visible sediment and stable colloidal fractions composed of polymeric nanoparticles, as confirmed by infrared spectroscopy, electron microscopy (Fig. 1a) and optical profilometry (Fig. 1b). These findings point to a direct mechanism of NMP generation, separate from material weathering, and raise concerns regarding waste management practices in small- and large-scale 3D printing environments.

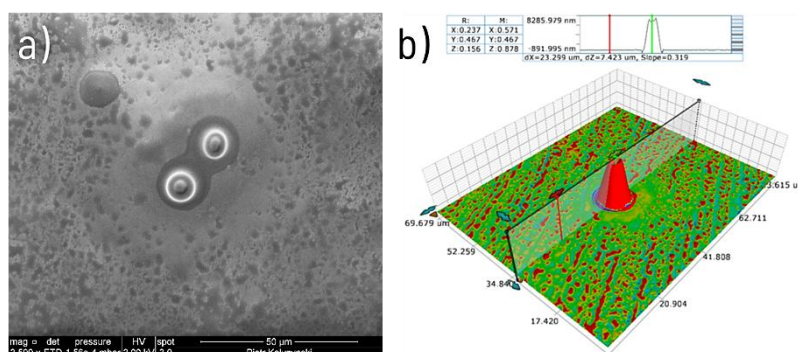


Fig. 1 (a) SEM of microplastic from 3D printing resin. (b) Optical profilometry of microplastic from 3D printing resin.

Beyond environmental release, concerns also arise regarding the biocompatibility of printed objects themselves. Cytotoxic effects of various photopolymer resins and their wash effluents were assessed via MTT assays employing human keratinocyte (HaCaT) cell models. Results indicate that standard curing protocols do not necessarily eliminate the leaching of biologically active compounds, with certain resins eliciting significant reductions in cell viability. These outcomes underscore the inadequacy of current post-processing protocols in mitigating toxicological risks for materials intended for skin or incidental food contact.

To address these risks, we evaluated the use of an SU8 photoresist layer as a post-print surface barrier. This epoxy-based coating, widely used in microfabrication, demonstrated promising potential in reducing direct exposure to residual monomers and enhancing surface biostability.

Taken together, our results highlight two interlinked challenges in polymer-based additive manufacturing: the inadvertent generation of NMPs and insufficient post-processing to ensure user and environmental safety. A holistic approach – integrating material reformulation, process optimization, and surface engineering – is therefore essential to advancing safer and more sustainable applications of 3D printing technologies.

Funding and acknowledgements. This work was supported by IDUB Programme (Program Inicjatywa Doskonałości - Uczelnia Badawcza) – Silesian University of Technology, Student Chapters Scientific Projects.

Micro modifications of hollow-core fibers using femtosecond laser pulses and focused ion beam

Patrycja Gronowicz^{1,2}, Michał Nikodem¹, Krzysztof Palka²

¹ Department of Optics and Photonics, Wrocław University of Science and Technology, Wybrzeże Wyspiańskiego 27, 50-370 Wrocław, Poland

² Whitecarbon/Nanores, Bierutowska 57-59, 51-317 Wrocław, Poland

Corresponding author: patrycja.gronowicz@pwr.edu.pl

Optical fibers with micro- and nanoscale modifications are increasingly used to enhance sensitivity, detectability, response time, durability, and safety in sensing applications [1]. Despite their potential, precise and repeatable optical fibers modification presents significant challenges, particularly when creating small structures. In our work we explore advanced methods for modifying hollow-core optical fibers at the micro- and nanoscale using a focused ion beam (FIB) in a SEM/PFIB microscope (Fig. 1) and a femtosecond laser (Fig. 2).

During the conference we will demonstrate the possibilities and challenges of micro modifications of anti-resonant hollow-core optical fibers using focused ion beam and femtosecond laser. Advantages and drawbacks of each technique will be presented and discussed. While modifications made using femtosecond laser pulses are have already been reported (e.g. [1]) we will focus primarily on focused ion beam.

Furthermore, we will also present how these modifications can help reducing the complexity of the gas detection systems that use hollow-core fibers as gas cells [2].

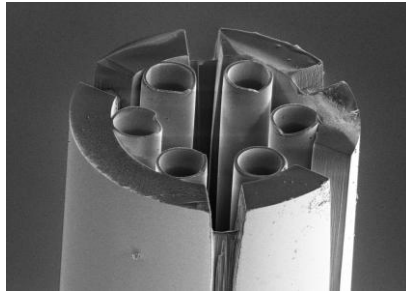


Fig. 1. Example of micromodifications (side-holes) of the anti-resonant hollow-core fiber made with a focused ion beam.



Fig. 2. Example of micromodifications (a side-hole along the length of the hollow-core fiber) made by a femtosecond laser beam.

Funding and acknowledgements. This work was supported by the Ministry of Science and Education, Poland, program ‘Doktorat Wdrozeniowy’ (DWD/6/0556/2022).

References

- [1] P. Gronowicz, G. Gomółka, D. Pysz, R. Buczyński, M. Nikodem. “Demonstration of a compact reflective gas sensing probe based on negative hollow-core fiber”. *Applied Optics* (2025).
- [2] P. Kozioł, P. Bojęś, P. Jaworski, D. Wu, F. Yu, K. Krzempek, “Enhancing Gas Diffusion in Antiresonant Hollow-Core Fiber Gas Sensors Using Microchannels”, *Photonic Sensors* 15, 250336 (2025).